



A THEORY OF FINITE VISCOELASTICITY AND NUMERICAL ASPECTS

STEFANIE REESE* and SANJAY GOVINDJEE

Structural Engineering, Mechanics and Materials, Department of Civil and Environmental Engineering, University of California at Berkeley, Berkeley, CA 94720-1710, U.S.A.

(Received 27 July 1996; in revised form 10 July 1997)

Abstract—Most current models for finite deformation viscoelasticity are restricted to linear evolution laws for the viscous material behaviour. In this paper, we present a model for finite deformation viscoelasticity that utilizes a nonlinear evolution law, and thus is not restricted to states close to the thermodynamic equilibrium. We further show that upon appropriate linearization, we can recover several established models of finite linear viscoelasticity and linear viscoelasticity. The utilization of this model in a computational setting is also addressed and examples are presented to highlight the differences of the proposed model in relation with other available models. © 1998 Elsevier Science Ltd. All rights reserved.

1. INTRODUCTION

Many materials simultaneously exhibit elastic and viscous material behaviour, a common example being polymeric materials. The goal of this paper is to develop a theory which accounts for the combination of elastic and viscous material behaviour at large deformations. Due to the high deformability of polymers, one must consider large deformation mechanics. In this framework, a common simplification when dealing with viscous materials is to restrict the formulation to small perturbations away from thermodynamic equilibrium, which is defined as usual by the vanishing of rate quantities. A viscoelastic solid under constant stress reaches such a state when the creep process in the system is completed. Taking into account only small perturbations away from thermodynamic equilibrium means that the system is not allowed to creep noticeably or, in other words, the strain rate has to be close to zero. Since large deformations are considered, this represents a fairly strong restriction of a material model for viscoelasticity. Furthermore, an assumption of this kind is not justified by means of a comparison with experiments. To avoid this difficulty, this paper contains a theory valid for deviations of any size away from thermodynamic equilibrium, i.e. valid for large deformation rates. The theory is simple enough to be implemented in a finite element code and for states close to the thermodynamic equilibrium we recover by linearization of the general theory several known formulations.

The kinetic theory of elasticity (see e.g. Treloar, 1943a, b; James and Guth, 1943, 1949) represents a self-consistent molecular theory for rubbers showing rate-independent elastic material behaviour. Using the result from this theory that the stiffness is proportional to the concentration of network chains, Green and Tobolsky (1946) were able to extend this theory to include relaxation effects. They explained the decay of stress at constant extension by the assumption that the formation of new bonds and the breakage of old bonds may decrease the stress in stretched chains. Incorporating this mechanism in the kinetic theory led them to linear differential equations for strain-like internal variables describing the “internal strain” of a chain. Based on Green and Tobolsky (1946), Lubliner (1985) split the free energy of a viscoelastic solid in two parts: the first part describing the rate-independent material behaviour and the second incorporating time-dependent effects. He further assumed a multiplicative decomposition of the deformation gradient into elastic and inelastic parts and interpreted Green and Tobolsky’s internal strain as inelastic strain.

* Author to whom correspondence should be addressed. Permanent address: Institute of Mechanics (IV), Technische Hochschule Darmstadt, Hochschulstr. 1, D-64289 Darmstadt, Germany.

The multiplicative decomposition of the deformation gradient, originally suggested by Lee (see e.g. Lee, 1969) in the context of elastoplasticity, has also been applied in nonlinear viscoelasticity by Sidoroff (1974).

An important point in developing models of this form is the choice of the evolution equation for the internal variables. In the theory of linear viscoelasticity, which is only valid for small deformations and small perturbations away from thermodynamic equilibrium, one can take either the “over-stress” or the inelastic strain as an internal variable. Due to the fact that the relationship between these two is linear and additionally all stress and strain measures coincide for small deformations, the structure of the evolution equation is evident (see e.g. the textbook of Tschoegl, 1989). In the case of large deformations, however, the choice of internal variables and evolution equations is not so evident and not unique. We can subdivide the theories for viscoelasticity combined with large deformations into two groups. We will speak of finite linear viscoelasticity when small deviations away from thermodynamic equilibrium are assumed. Evolution equations belonging to this kind of theory are linear differential equations with possibly non-constant coefficients (e.g. a deformation-dependent relaxation time). The term finite viscoelasticity is reserved for theories which account for large perturbations away from the equilibrium state and thus are more general.

Examples of finite linear viscoelasticity would include the works of Coleman and Noll (1961), Valanis (1966), Crochet and Naghdi (1969), Christensen (1980), Lubliner (1985), Le Tallec *et al.* (1993) and Dafalias (1991). One of the first finite element implementations for such a theory was given by Simo (1987). In contrast to most works, however, he chose the over-stress as the internal variable. This approach was also followed by Govindjee and Simo (1992, 1993), Holzapfel (1996) and Kaliske and Rothert (1997). Theories for finite viscoelasticity are discussed for example in Koh and Eringen (1963), Sidoroff (1974) and Haupt (1993a, b). This latter work was developed by Lion (1996b) into a practically usable finite viscoelastic material model and to fit experimental results.

In this paper we propose an additive split of the free energy into an equilibrium and a non-equilibrium part. The concept is based on a multiplicative decomposition of the deformation gradient into an elastic and an inelastic part. A theory of this kind has already been presented by Lubliner (1985), but we will extend his approach to finite viscoelasticity. The existence of a non-equilibrium free energy leads to a non-equilibrium stress which can be derived from a potential. It is evident that this assumption does not hold for every viscoelastic material, but for rubber-like materials at least, it should be reasonable. This hypothesis is supported by the results of Lion (1996a, b), whose theory is also based on this assumption and who obtained excellent correlation with experimental results.

In the first section of this paper, we develop a theory for finite viscoelasticity, which is consistent with the internal variable framework in Coleman and Gurtin (1967). For the case of isotropy, we show that, upon linearization about thermodynamic equilibrium, we recover Lubliner’s model of finite linear viscoelasticity. Further, it will be demonstrated that, by considering small deformations, we recover from our general theory the standard linear solid of infinitesimal viscoelasticity.

One advantage of the presented formulation is that it can be easily implemented in a finite element code (Sections 2 and 3). This is due to the fact that the evolution equation of finite viscoelasticity derived in this work has the same structure as the one used in finite deformation associative elastoplasticity (Simo and Miehe, 1992) and viscoplasticity (Simo, 1992). Thus, the time integration can be carried out by the exponential mapping algorithm (see Weber and Anand, 1990; Cuitino and Ortiz, 1992; Simo, 1992), which up to now has only been used in computational elastoplasticity and viscoplasticity. As in elastoplasticity, we obtain for the linearized theory an integration algorithm linear in the logarithmic principal values of a kinematic measure. The solution of the weak form of equilibrium is described in Section 3. It is shown that, due to the derivation of the over-stress from a potential and the special form chosen for the evolution equation, we arrive at a symmetric tangent operator. The paper concludes with some examples which show the applicability of the proposed theory and the necessity of being able to account for large perturbations away from thermodynamic equilibrium in a theory of viscoelasticity.

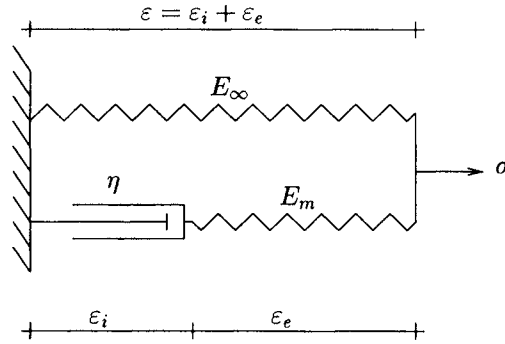


Fig. 1. Rheological model for linear viscoelastic material behaviour.

2. CONSTITUTIVE EQUATIONS

2.1. General theory

To derive the constitutive equations for the materials of interest, we begin with a Helmholtz free energy function per unit reference volume:

$$\Psi = \hat{\Psi}(\mathbf{C}, \mathbf{Q}_1, \mathbf{Q}_2, \dots, \mathbf{Q}_n). \quad (1)$$

Due to the principle of objectivity, it reduces to a function of the right Cauchy–Green tensor \mathbf{C} plus a set of n internal variables \mathbf{Q}_k , $k = 1, 2, \dots, n$ (see e.g. Coleman and Gurtin, 1967). To determine the internal variables, a set of n evolution equations of the form

$$\dot{\mathbf{Q}}_k = \hat{\mathbf{f}}_k(\mathbf{C}, \mathbf{Q}_1, \dots, \mathbf{Q}_n) \quad (2)$$

are needed. The constitutive equations are further required to fulfil the entropy inequality, which, if only isothermal processes are considered, is equal to the so-called internal dissipation inequality

$$\frac{1}{2} \mathbf{S} : \dot{\mathbf{C}} - \dot{\Psi} \geq 0, \quad (3)$$

where

$$\mathbf{S} = \hat{\mathbf{S}}(\mathbf{C}, \mathbf{Q}_1, \mathbf{Q}_2, \dots, \mathbf{Q}_n) \quad (4)$$

is the second Piola–Kirchhoff stress tensor. Employing (1), (3) reduces to

$$\left(\mathbf{S} - 2 \frac{\partial \Psi}{\partial \mathbf{C}} \right) : \frac{1}{2} \dot{\mathbf{C}} - \sum_{k=1}^n \frac{\partial \Psi}{\partial \mathbf{Q}_k} : \dot{\mathbf{Q}}_k \geq 0. \quad (5)$$

To proceed further, we first consider the common small deformation case, schematically shown in Fig. 1.

In this case, the total stress is given by

$$\sigma = \underbrace{E_\infty \varepsilon}_{\sigma_{EQ}} + \underbrace{E_m \varepsilon_e}_{\sigma_{NEQ}} \quad (6)$$

or alternatively by

$$\sigma = \underbrace{\frac{\partial}{\partial \varepsilon} \left(\frac{1}{2} E_\infty \varepsilon^2 \right)}_{\hat{\sigma}_{EQ}(\varepsilon)} + \underbrace{\frac{\partial}{\partial \varepsilon_e} \left(\frac{1}{2} E_m \varepsilon_e^2 \right)}_{\hat{\sigma}_{NEQ}(\varepsilon_e)}. \quad (7)$$

The latter equation motivates the additive split of the free energy into two parts:

$$\Psi = \hat{\Psi}(\varepsilon, \varepsilon_e) = \underbrace{\frac{1}{2} E_\infty \varepsilon^2}_{\hat{\Psi}_{EQ}(\varepsilon)} + \underbrace{\frac{1}{2} E_m \varepsilon_e^2}_{\hat{\Psi}_{NEQ}(\varepsilon_e)}. \quad (8)$$

In the rheological model, Ψ_{EQ} represents the strain energy in the “time-infinity” spring and Ψ_{NEQ} the strain energy in the Maxwell element. In the thermodynamic equilibrium state the spring of the Maxwell element is relaxed ($\varepsilon_e = 0$), i.e. the total free energy consists only of the equilibrium part Ψ_{EQ} .

The preceding considerations motivate the ansatz

$$\Psi = \hat{\Psi}_{EQ}(\mathbf{C}) + \hat{\Psi}_{NEQ}(\mathbf{C}_e), \quad (9)$$

where \mathbf{C}_e represents the “elastic” right Cauchy–Green tensor; loosely speaking, \mathbf{C}_e is the strain associated with the spring in the Maxwell element in Fig. 1. The precise definition follows from the multiplicative split of the total deformation gradient

$$\mathbf{F} = \mathbf{F}_e \cdot \mathbf{F}_i \quad (10)$$

into an elastic part \mathbf{F}_e and an inelastic (or viscous) part \mathbf{F}_i which can be viewed as the deformation gradient associated with the dashpot in Fig. 1. The tensor \mathbf{C}_e is then defined by $\mathbf{C}_e = \mathbf{F}_e^T \cdot \mathbf{F}_e$. In finite viscoelasticity, similar concepts have been employed by Sidoroff (1974), Lubliner (1985), Le Tallec *et al.* (1993) and Lion (1996b).

In order for (9) to be formally consistent with (1) and (3), the free energy is specified as a function of \mathbf{C} and \mathbf{F}_i , i.e.

$$\Psi = \hat{\Psi}(\mathbf{C}, \mathbf{F}_i) = \hat{\Psi}_{EQ}(\mathbf{C}) + \hat{\Psi}_{NEQ}(\mathbf{F}_i^{-T} \cdot \mathbf{C} \cdot \mathbf{F}_i^{-1}). \quad (11)$$

Note that $\mathbf{C}_e = \mathbf{F}_i^{-T} \cdot \mathbf{C} \cdot \mathbf{F}_i^{-1}$. With this modified ansatz one finds that the dissipation inequality (5) reduces to

$$\left(\mathbf{S} - 2 \frac{\partial \Psi_{EQ}}{\partial \mathbf{C}} - 2 \mathbf{F}_i^{-1} \cdot \frac{\partial \Psi_{NEQ}}{\partial \mathbf{C}_e} \cdot \mathbf{F}_i^{-T} \right) : \frac{1}{2} \dot{\mathbf{C}} - \frac{\partial \Psi_{NEQ}}{\partial \mathbf{C}_e} : \frac{\partial \mathbf{C}_e}{\partial \mathbf{F}_i} : \dot{\mathbf{F}}_i \geq 0. \quad (12)$$

By the argument of Coleman and Gurtin (1967), the stress is then given by

$$\mathbf{S} = \mathbf{S}_{EQ} + \mathbf{S}_{NEQ} = \underbrace{2 \frac{\partial \Psi_{EQ}}{\partial \mathbf{C}}}_{\mathbf{S}_{EQ}} + \underbrace{2 \mathbf{F}_i^{-1} \cdot \frac{\partial \Psi_{NEQ}}{\partial \mathbf{C}_e} \cdot \mathbf{F}_i^{-T}}_{\mathbf{S}_{NEQ}} = 2 \frac{\partial \Psi}{\partial \mathbf{C}}. \quad (13)$$

Remark 1: In the following, we assume that Ψ_{EQ} and Ψ_{NEQ} are chosen in such a way that in the thermodynamic equilibrium \mathbf{S}_{NEQ} and Ψ_{NEQ} disappear.

By utilizing (13) in (12), the residual inequality gives

$$\frac{\partial \Psi_{NEQ}}{\partial \mathbf{C}_e} : (\mathbf{l}_i^T \cdot \mathbf{C}_e + \mathbf{C}_e \cdot \mathbf{l}_i) \geq 0, \quad (14)$$

or, by exploiting the symmetry properties,

$$2 \frac{\partial \Psi_{NEQ}}{\partial \mathbf{C}_e} : (\mathbf{C}_e \cdot \mathbf{l}_i) \geq 0, \quad (15)$$

where $\mathbf{l}_i = \dot{\mathbf{F}}_i \cdot \mathbf{F}_i^{-1}$ is termed the inelastic part of the spatial velocity gradient $\mathbf{l} = \dot{\mathbf{F}} \cdot \mathbf{F}^{-1}$.

Rewriting (15) in the form

$$2 \mathbf{F}_e \cdot \frac{\partial \Psi_{NEQ}}{\partial \mathbf{C}_e} \cdot \mathbf{F}_e^T : (\mathbf{F}_e^{-T} \cdot \mathbf{C}_e \cdot \mathbf{l}_i \cdot \mathbf{F}_e^{-1}) \geq 0 \quad (16)$$

leads to

$$\boldsymbol{\tau}_{NEQ} \cdot \mathbf{b}_e^{-1} : (\mathbf{F}_e \cdot \mathbf{l}_i \cdot \mathbf{F}_e^T) \geq 0, \quad (17)$$

where the relations

$$\boldsymbol{\tau}_{NEQ} = 2 \mathbf{F}_e \cdot \frac{\partial \Psi_{NEQ}}{\partial \mathbf{C}_e} \cdot \mathbf{F}_e^T \quad \text{and} \quad \mathbf{b}_e = \mathbf{F}_e \cdot \mathbf{F}_e^T \quad (18)$$

have been used. Furthermore, one finds that $\mathbf{F}_e \cdot \mathbf{l}_i \cdot \mathbf{F}_e^T$ can be written as

$$\mathbf{F}_e \cdot \mathbf{l}_i \cdot \mathbf{F}_e^T = -\frac{1}{2} \underbrace{\mathbf{F} \cdot (\dot{\mathbf{C}}_i^{-1}) \cdot \mathbf{F}^T}_{\mathcal{L}_v \mathbf{b}_e} + \text{skw}(\mathbf{F}_e \cdot \mathbf{l}_i \cdot \mathbf{F}_e^T). \quad (19)$$

Here, the notation $\mathcal{L}_v \mathbf{b}_e$ stands for the Lie derivative of the contravariant tensor \mathbf{b}_e and $\mathbf{C}_i = \mathbf{F}_i^T \cdot \mathbf{F}_i$ denotes the “inelastic” right Cauchy–Green tensor. Equations (16)–(19) apply in the general anisotropic case. But now we assume isotropy and consequently Ψ_{NEQ} to be an isotropic tensor function. Therefore, we may write $\hat{\Psi}_{NEQ}(\mathbf{b}_e)$. In this case $\boldsymbol{\tau}_{NEQ}$ and \mathbf{b}_e commute, which gives the symmetry of the tensor $\boldsymbol{\tau}_{NEQ} \cdot \mathbf{b}_e^{-1}$. Thus, in inequality (17) only the symmetric part of $\mathbf{F}_e \cdot \mathbf{l}_i \cdot \mathbf{F}_e^T$ plays a role and we come to the well-known residual (isotropic) inequality

$$-\boldsymbol{\tau}_{NEQ} : \frac{1}{2} (\mathcal{L}_v \mathbf{b}_e) \cdot \mathbf{b}_e^{-1} \geq 0; \quad (20)$$

for an alternative derivation based on different assumptions, see e.g. Simo and Miehe (1992).

A sufficient condition fulfilling (20) is to make it a positive definite quadratic form. This natural choice gives the evolution equation

$$-\frac{1}{2} \mathcal{L}_v \mathbf{b}_e \cdot \mathbf{b}_e^{-1} = \mathcal{V}^{-1} : \boldsymbol{\tau}_{NEQ}, \quad (21)$$

where $\mathcal{V}^{-1} = \hat{\mathcal{V}}^{-1}(\mathbf{b}_e)$ is an isotropic rank four tensor which has to be positive definite to satisfy (20). In this case, \mathcal{V}^{-1} takes the form (see e.g. Gurtin, 1991, Section 37 or Fung, 1994, Section 8.4):

$$\mathcal{V}^{-1} = \frac{1}{2\eta_D} \left(\mathbf{1}^4 - \frac{1}{3} \mathbf{1} \otimes \mathbf{1} \right) + \frac{1}{9\eta_V} \mathbf{1} \otimes \mathbf{1}. \quad (22)$$

Here, $\mathbf{1}^4$ is the fourth order symmetric identity tensor, while η_D and η_V represent the deviatoric and volumetric viscosities, respectively. They are possibly deformation dependent and have the following properties:

$$\eta_D = \hat{\eta}_D(\mathbf{b}_e) > 0, \quad \hat{\eta}_D(\mathbf{1}) = \eta_{DEQ}, \quad (23)$$

$$\eta_V = \hat{\eta}_V(\mathbf{b}_e) > 0, \quad \hat{\eta}_V(\mathbf{1}) = \eta_{VEQ}. \quad (24)$$

If (22) is inserted in evolution equation (21), then we obtain

$$-\mathcal{L}_v \mathbf{b}_e \cdot \mathbf{b}_e^{-1} = \frac{1}{\eta_D} \text{dev} [\boldsymbol{\tau}_{NEQ}] + \frac{2}{9\eta_V} (\boldsymbol{\tau}_{NEQ} : \mathbf{1}) \mathbf{1}. \quad (25)$$

Note, the right side of the latter equation can only vanish, if $\boldsymbol{\tau}_{NEQ} = \mathbf{0}$, which implies $\mathbf{b}_e = \mathbf{1}$ as desired.

Remark 2: The model developed is also intimately related to the “plasticity” model of Boyce *et al.* (1988). In fact, we recover their model by choosing $\eta_V = 0$ and η_D as a function of $\|\text{dev} \boldsymbol{\tau}_{NEQ}\|$. Thus, we can also interpret the model of Boyce *et al.* (1988) as a viscoelasticity model and conclude that it, too, satisfies the Clausius–Duhem inequality.

2.2. Linearized theories

In this subsection, we discuss the reduction of the presented theory to a theory of linear viscoelasticity. That such a reduction is possible is a natural requirement for any nonlinear large deformation viscoelastic model. This requires two linearization steps. In the first step we linearize about thermodynamic equilibrium $\mathbf{b}_e = \mathbf{1}$. The resulting theory is still valid for large deformations but is restricted to the case that $\mathbf{b}_e \approx \mathbf{1}$, i.e. to small perturbations away from thermodynamic equilibrium. For the rheological model presented in Fig. 1 this means that the spring in the Maxwell element is nearly relaxed. A theory of this kind is called “finite linear” viscoelasticity; we will show that our model restricted to the range of finite linear viscoelasticity is nearly identical to the finite linear theory proposed by Lubliner (1985). In the second step, we carry out a linearization about the undeformed reference configuration. In this way, we develop a model which is valid only for $\mathbf{b}_e \approx \mathbf{1}$ and small deformations ($\mathbf{b} \approx \mathbf{1}$).

We begin by linearizing (21) about $\mathbf{b}_e = \mathbf{1}$:

$$\begin{aligned} -\frac{1}{2}(\mathcal{L}_v \mathbf{b}_e \cdot \mathbf{b}_e^{-1})_{\text{lin}} &= [\boldsymbol{\gamma}^{-1} : \boldsymbol{\tau}_{NEQ}]_{EQ} \\ &+ \left(\left[\frac{\partial \boldsymbol{\gamma}^{-1}}{\partial \mathbf{b}_e} : \boldsymbol{\tau}_{NEQ} \right]_{EQ} + \left[\boldsymbol{\gamma}^{-1} : \frac{\partial \boldsymbol{\tau}_{NEQ}}{\partial \mathbf{b}_e} \right]_{EQ} \right) : (\mathbf{b}_e - \mathbf{1}) \\ &= \left[\boldsymbol{\gamma}^{-1} : \frac{\partial \boldsymbol{\tau}_{NEQ}}{\partial \mathbf{b}_e} \right]_{EQ} : \frac{1}{2}(\mathbf{b}_e - \mathbf{1}), \end{aligned} \quad (26)$$

where we have taken advantage of the fact that

$$[\boldsymbol{\tau}_{NEQ}]_{EQ} = \mathbf{0}. \quad (27)$$

The term $2[\partial \boldsymbol{\tau}_{NEQ} / \partial \mathbf{b}_e]_{EQ}$ is calculated as follows:

$$\begin{aligned}
2 \left[\frac{\partial \boldsymbol{\tau}_{NEQ}}{\partial \mathbf{b}_e} \right]_{EQ} &= 2 \left[\frac{\partial}{\partial \mathbf{b}_e} \left(2 \frac{\partial \Psi_{NEQ}}{\partial \mathbf{b}_e} \cdot \mathbf{b}_e \right) \right]_{EQ} \\
&= \left[4 \frac{\partial^2 \Psi_{NEQ}}{\partial \mathbf{b}_e \otimes \partial \mathbf{b}_e} \cdot \mathbf{b}_e + 4 \frac{\partial \Psi_{NEQ}}{\partial \mathbf{b}_e} \cdot \mathbf{1}^4 \right]_{EQ} \\
&= \left[4 \mathbf{b}_e \cdot \frac{\partial^2 \Psi_{NEQ}}{\partial \mathbf{b}_e \otimes \partial \mathbf{b}_e} \cdot \mathbf{b}_e + 4 \underbrace{\frac{\partial \Psi_{NEQ}}{\partial \mathbf{b}_e} \cdot \mathbf{b}_e \cdot \mathbf{1}^4}_{\frac{1}{2} \boldsymbol{\tau}_{NEQ}} \right]_{EQ} \quad (28)
\end{aligned}$$

$$= \left[4 \mathbf{b}_e \cdot \frac{\partial^2 \Psi_{NEQ}}{\partial \mathbf{b}_e \otimes \partial \mathbf{b}_e} \cdot \mathbf{b}_e \right]_{EQ} = \mathcal{C}. \quad (29)$$

The multiplication with \mathbf{b}_e in (28) does not change the equation, since in thermodynamic equilibrium $\mathbf{b}_e = \mathbf{1}$. Note that the rank four tensor \mathcal{C} is identical in form to the constitutive tensor derived in isotropic finite elasticity with respect to the current configuration (see e.g. Miehe, 1994, 1995). It, too, has the well-known structure

$$\mathcal{C} = 2\mu_m(\mathbf{1}^4 - \frac{1}{3}\mathbf{1} \otimes \mathbf{1}) + K_m\mathbf{1} \otimes \mathbf{1}, \quad (30)$$

where the shear modulus μ_m and the bulk modulus K_m are to be interpreted as material constants of the non-equilibrium part of the viscoelastic material model. In the one-dimensional rheological model shown in Fig. 1 these are represented by the stiffness E_m of the spring in the Maxwell element.

If (30) is combined with (26), the linearized evolution equation becomes

$$\boxed{-\frac{1}{2}(\mathcal{L}_v \mathbf{b}_e \cdot \mathbf{b}_e^{-1})_{\text{lin}} = \frac{1}{2\tau}(\mathbf{b}_e - \mathbf{1})}, \quad (31)$$

where τ denotes the near thermodynamic equilibrium relaxation time of the system and is given by $\tau = \eta_{DEQ}/\mu_m = \eta_{VEQ}/K_m$. By use of the definition of the Lie derivative, we come to the alternative representation

$$\dot{\mathbf{C}}_i^{-1} = \frac{1}{\tau}(\mathbf{C}_i^{-1} - \mathbf{C}_i^{-1} \cdot \mathbf{C} \cdot \mathbf{C}_i^{-1}) = \frac{1}{\tau} \mathbf{C}_i^{-1} \cdot \mathbf{C} \cdot (\mathbf{C}^{-1} - \mathbf{C}_i^{-1}). \quad (32)$$

For states close to the thermodynamic equilibrium we have

$$\mathbf{C}_i^{-1} \cdot \mathbf{C} \approx \mathbf{1} + \mathbf{A}, \quad (33)$$

where the norm of \mathbf{A} is small with respect to the norm of the identity tensor. Ignoring the terms associated with \mathbf{A} gives

$$\dot{\mathbf{C}}_i^{-1} = \frac{1}{\tau}(\mathbf{C}^{-1} - \mathbf{C}_i^{-1}), \quad (34)$$

which is exactly the evolution equation of Lubliner (1985). Thus, we properly recover Lubliner's large deformation linear viscoelasticity theory. Other finite linear theories can be obtained in a similar manner.

To examine the small deformation case we define the linearized Green–Lagrange strain tensor

$$(\mathbf{E})_{\text{lin}} = \frac{1}{2}(\mathbf{C} - \mathbf{1})_{\text{lin}} \quad (35)$$

and $[(\mathbf{E})_{\text{lin}}]_e = (\mathbf{E})_{\text{lin}} - [(\mathbf{E})_{\text{lin}}]_i$, where $[(\mathbf{E})_{\text{lin}}]_i = \frac{1}{2}(\mathbf{C}_i - \mathbf{1})_{\text{lin}}$. With these definitions in hand (32) reduces to

$$\overline{[(\mathbf{E})_{\text{lin}}]_i} = \frac{1}{\tau} [(\mathbf{E})_{\text{lin}}]_e. \quad (36)$$

This expression is easily seen to be the governing relation for a linear Maxwell rheological element from the small deformation theory. Note that in deriving (36) it is useful to first rewrite (32) in the equivalent form

$$\frac{1}{2}\dot{\mathbf{C}}_i = \frac{1}{2\tau}(\mathbf{C} - \mathbf{C}_i). \quad (37)$$

Remark 3: In summary, the evolution eqn (36) is valid for small deformations and small deviations away from thermodynamic equilibrium. Thus, one is restricted to the range of linear viscoelasticity theory. Using (31) or equivalently (37) allows large deformations, but only small deviations away from thermodynamic equilibrium are permitted, i.e. finite linear viscoelasticity theory. The general eqn (21) is valid for large deformations and large perturbations away from thermodynamic equilibrium, i.e. finite viscoelasticity. A similar evolution equation was derived by Lion (1996b), who, however, used the same viscosity for the volumetric and the deviatoric parts. Certainly, (21) is not the only possible form which satisfies (20), but as will be seen, it has several attractive properties from a computational point of view.

In the next section we will discuss the algorithm used for the integration of an evolution equation of the form (21).

3. INTEGRATION OF THE EVOLUTION EQUATION

3.1. Operator split: isotropy

For the purpose to show that the evolution equation (21) has potential character we rewrite it in the form

$$-\frac{1}{2}\mathcal{L}_v \mathbf{b}_e \cdot \mathbf{b}_e^{-1} = \frac{1}{\tau} \frac{\partial}{\partial \tau_{NEQ}} \left(\frac{\tau}{2} \tau_{NEQ} : \mathcal{V}^{-1} : \tau_{NEQ} \right) = \frac{1}{\tau} \frac{\partial \Phi_{\text{vis}}}{\partial \tau_{NEQ}} \quad (38)$$

(see also Appendix C). Φ_{vis} can be interpreted as a so-called creep potential. An algorithm for the integration of evolution equations of this form has been proposed by Weber and Anand (1990), Cuitino and Ortiz (1992) and Simo (1992) in the context of elastoplasticity. The main feature of these algorithms is to carry out an operator split of the material time derivative of \mathbf{b}_e into an elastic predictor E and an inelastic corrector I :

$$\dot{\mathbf{b}}_e = \overline{(\mathbf{F} \cdot \mathbf{C}_i^{-1} \cdot \mathbf{F}^T)} = \underbrace{\mathbf{1} \cdot \mathbf{b}_e + \mathbf{b}_e \cdot \mathbf{1}^T}_E + \underbrace{\mathbf{F} \cdot (\mathbf{C}_i^{-1}) \cdot \mathbf{F}^T}_I. \quad (39)$$

The main objective here is to determine in an efficient manner the value of the governing inelastic internal variable for an advancement of time in order that the stresses may be evaluated when the material motion is known—the typical setting in a finite element program for instance. In the elastic predictor step the material time derivative of \mathbf{C}_i^{-1} is set to zero. Therefore we have

$$(\mathbf{C}_i^{-1})_{\text{trial}} = (\mathbf{C}_i^{-1})_{t=t_{n-1}} \Rightarrow (\mathbf{b}_e)_{\text{trial}} = (\mathbf{F})_{t=t_n} \cdot (\mathbf{C}_i^{-1})_{t=t_{n-1}} \cdot (\mathbf{F})_{t=t_n}^T. \quad (40)$$

In analogy to elastoplasticity, the state calculated with the elastic predictor step is called the trial state.

In the inelastic corrector step, the spatial velocity gradient is set to zero, which leads to $\mathcal{L}_v \mathbf{b}_e = \dot{\mathbf{b}}_e$ and finally to

$$\dot{\mathbf{b}}_e = -(2\mathcal{V}^{-1} : \boldsymbol{\tau}_{NEQ}) \cdot \mathbf{b}_e. \quad (41)$$

Solving the differential equation by the so-called exponential mapping gives

$$\mathbf{b}_e = \exp \left[-2 \int_{t_{n-1}}^t \mathcal{V}^{-1} : \boldsymbol{\tau}_{NEQ} dt \right] \cdot (\mathbf{b}_e)_{\text{trial}}, \quad (42)$$

$$(\mathbf{b}_e)_{t=t_n} \approx \exp \left[-2 \underbrace{(t_n - t_{n-1})}_{\Delta t} (\mathcal{V}^{-1} : \boldsymbol{\tau}_{NEQ})_{t=t_n} \right] \cdot (\mathbf{b}_e)_{\text{trial}}. \quad (43)$$

The approximate expression on the right hand side is first order accurate.

Due to isotropy, $\boldsymbol{\tau}_{NEQ}$ commutes with \mathbf{b}_e and also with $(\mathbf{b}_e)_{\text{trial}}$ (see Appendix A). Since \mathcal{V}^{-1} is assumed to be isotropic, we can write (43) in principal axes. For the finite viscoelastic evolution (21) this leads to

$$\lambda_{Ae}^2 = \exp \left[-\Delta t \left(\frac{1}{\eta_D} \text{dev} [\boldsymbol{\tau}_A] + \frac{2}{9\eta_V} \boldsymbol{\tau}_{NEQ} : \mathbf{1} \right) \right] (\lambda_{Ae}^2)_{\text{trial}}, \quad (44)$$

where $\text{dev} [\boldsymbol{\tau}_A]$ are the principal values of $\text{dev} [\boldsymbol{\tau}_{NEQ}]$, λ_{Ae}^2 the principal values of $(\mathbf{b}_e)_{t=t_n}$ and $(\lambda_{Ae}^2)_{\text{trial}}$ the principal values of $(\mathbf{b}_e)_{\text{trial}}$. Taking the logarithm of both sides yields

$$\varepsilon_{Ae} = -\Delta t \left(\frac{1}{2\eta_D} \text{dev} [\boldsymbol{\tau}_A] + \frac{1}{9\eta_V} \boldsymbol{\tau}_{NEQ} : \mathbf{1} \right) + (\varepsilon_{Ae})_{\text{trial}}, \quad (45)$$

where $\varepsilon_{Ae} = \ln \lambda_{Ae}$ are the elastic logarithmic principal stretches. In evaluating the constitutive law for $\boldsymbol{\tau}_A$ (see Section 2.3), (45) furnishes an implicit nonlinear equation for determining the principal values of \mathbf{b}_e ; note, the non-equilibrium Kirchhoff stresses depend on these values.

3.2. Linearized case

For the finite linear viscoelastic evolution eqn (31) a similar derivation leads to

$$\lambda_{Ae}^2 = \exp \left[-\frac{\Delta t}{\tau} (\lambda_{Ae}^2 - 1) \right] (\lambda_{Ae}^2)_{\text{trial}} \quad (46)$$

and hence

$$\varepsilon_{Ae} = -\frac{\Delta t}{\tau} \frac{1}{2} (\lambda_{Ae}^2 - 1) + (\varepsilon_{Ae})_{\text{trial}}. \quad (47)$$

If one linearizes ε_{Ae} with respect to λ_{Ae}^2 around thermodynamic equilibrium $\lambda_{Ae}^2 = 1$, one obtains

$$(\varepsilon_{Ae})_{\text{lin}} = \left[\frac{\partial(\ln \lambda_{Ae})}{\partial(\lambda_{Ae}^2)} \right]_{EQ} (\lambda_{Ae}^2 - 1) = \frac{1}{2}(\lambda_{Ae}^2 - 1). \quad (48)$$

Since the evolution eqn (31) is only valid for small perturbations away from thermodynamic equilibrium, the linearization (48) does not represent any further restriction, and we can substitute (48) into (47) to give

$$\varepsilon_{Ae} = -\frac{\Delta t}{\tau} \varepsilon_{Ae} + (\varepsilon_{Ae})_{\text{trial}}, \quad (49)$$

where the subscripts “lin” have been dropped for convenience. Solving for ε_{Ae} gives us

$$\varepsilon_{Ae} = \left(1 + \frac{\Delta t}{\tau} \right)^{-1} (\varepsilon_{Ae})_{\text{trial}}, \quad (50)$$

which is seen to be an explicit updated formula for the logarithmic principal values of \mathbf{b}_e .

3.3. Local Newton iteration

In the case of isotropy the non-equilibrium free energy Ψ_{NEQ} can be represented as a function of the principal values $b_{Ae} = \lambda_{Ae}^2$ of \mathbf{b}_e , such that we obtain

$$\Psi_{NEQ} = \bar{\Psi}_{NEQ}(b_{1e}, b_{2e}, b_{3e}); \quad (51)$$

see e.g. Gurtin (1981, Section 37). It is not necessary but convenient to split both the non-equilibrium Kirchhoff stress tensor and the non-equilibrium part of the free energy into volumetric and deviatoric parts; thus, we write

$$\Psi_{NEQ} = \overline{(\Psi_{NEQ})_D}(\bar{b}_{1e}, \bar{b}_{2e}, \bar{b}_{3e}) + \overline{(\Psi_{NEQ})_V}(J_e). \quad (52)$$

Here,

$$J_e = \lambda_{1e} \lambda_{2e} \lambda_{3e} \quad (53)$$

denotes the determinant of \mathbf{F}_e and

$$\bar{b}_{Ae} = J_e^{-(2/3)} b_{Ae} = J_e^{-(2/3)} \lambda_{Ae}^2 \quad (54)$$

the principal values of

$$\bar{\mathbf{b}}_e = J_e^{-(2/3)} \mathbf{b}_e. \quad (55)$$

For the equilibrium and non-equilibrium parts of the material model, we work with the class of Ogden models (1972a, b) which is known to agree well with experimental results and to fulfil many mathematical requirements such as polyconvexity (Ball, 1977); see e.g. Treloar (1975) or Ogden (1972a, b). Considering the split into a deviatoric and a volumetric part, Ψ_{NEQ} takes the form

$$\Psi_{NEQ} = \underbrace{\sum_{r=1}^3 \frac{(\mu_m)_r}{(\alpha_m)_r} (\bar{b}_{1e}^{(\alpha_m)_r/2} + \bar{b}_{2e}^{(\alpha_m)_r/2} + \bar{b}_{3e}^{(\alpha_m)_r/2} - 3)}_{(\Psi_{NEQ})_D} + \underbrace{\frac{K_m}{4} (J_e^2 - 2 \ln J_e - 1)}_{(\Psi_{NEQ})_V}. \quad (56)$$

Here, $(\mu_m)_r$ and $(\alpha_m)_r$ are elasticity constants, such that for the shear modulus μ_m the relationship

$$\mu_m = \sum_{r=1}^3 \frac{1}{2} (\mu_m)_r (\alpha_m)_r \quad (57)$$

holds. For rubber-like materials we have $K_m \approx 1000 (\mu_m)_r$ (Ogden, 1972b), which means that the material behaviour is nearly incompressible.

The non-equilibrium part of the Kirchhoff stress tensor τ_{NEQ} is then given by the relation

$$\tau_{NEQ} = 2 \frac{\partial \Psi_{NEQ}}{\partial \mathbf{b}_e} \cdot \mathbf{b}_e = \sum_{A=1}^3 \tau_A \mathbf{n}_A \otimes \mathbf{n}_A = \sum_{A=1}^3 \frac{\partial \Psi_{NEQ}}{\partial \lambda_{Ae}} \lambda_{Ae} \mathbf{n}_A \otimes \mathbf{n}_A, \quad (58)$$

where the principal Kirchhoff stresses are calculated by

$$\tau_A = \underbrace{\sum_{B=1}^3 \frac{\partial (\Psi_{NEQ})_D}{\partial \bar{b}_{Be}} \frac{\partial \bar{b}_{Be}}{\partial \lambda_{Ae}} \lambda_{Ae}}_{\text{dev } \tau_A} + \underbrace{\frac{\partial (\Psi_{NEQ})_V}{\partial J_e} J_e}_{(1/3) \tau_{NEQ} : \mathbf{1}}. \quad (59)$$

It is now evident that with $\lambda_{Ae} = \exp [\varepsilon_{Ae}]$, (45) can be considered as a nonlinear equation in the elastic logarithmic stretches ε_{Ae} , whereas the linearized evolution (49) is solvable explicitly. In the nonlinear case, (45) is solved by means of a Newton iteration, which we will term a local Newton iteration, since it is needed for the calculation of the stresses. In a finite element context, this calculation has to be carried out at the Gauss point level. The Newton iteration is described in Table 1 below.

Remark 4: Note, Ψ_{NEQ} represents the strain energy in a single Maxwell element (see Fig. 1). To model the viscous behaviour of certain materials, it might be necessary to use several Maxwell elements in parallel instead of only one. In this case, we have to solve an evolution equation for each Maxwell element and obtain additional contributions to the non-equilibrium part of the Kirchhoff stress tensor. Using more Maxwell elements leads to a more elaborate calculation but does not represent any theoretical or numerical problems; see Govindjee and Reese (1997).

Table 1. Local Newton iteration

(1) Non-linear equation	$r_A = \varepsilon_{Ae} + \Delta t \left(\frac{1}{2\eta_D} \text{dev } \tau_A + \frac{1}{9\eta_V} \tau_{NEQ} : \mathbf{1} \right) - (\varepsilon_{Ae})_{\text{trial}} = 0$	(60)
(2) Linearize around $\varepsilon_{Ae} = (\varepsilon_{Ae})_k$	$r_A \approx \underbrace{r_A _{(\varepsilon_{Ae})_k}}_{(r_A)_k} + \sum_{B=1}^3 \underbrace{\frac{\partial r_A}{\partial \varepsilon_{Be}} \Big _{(\varepsilon_{Ae})_k}}_{(K_{AB})_k} (\Delta \varepsilon_{Be})_k = 0$	(61)
(3) Solve for $(\Delta \varepsilon_{Be})_k$	$\sum_{B=1}^3 (K_{AB})_k (\Delta \varepsilon_{Be})_k = -(r_A)_k$	(62)
Calculation of K_{AB} : see Appendix B		
(4) Update	$(\varepsilon_{Ae})_{k+1} = (\varepsilon_{Ae})_k + (\Delta \varepsilon_{Ae})_k, k \leftarrow k+1$	(63)
(5) Repeat until $\ r_A\ < \text{tol}$		

4. SOLUTION OF THE WEAK FORM OF EQUILIBRIUM

In a typical initial boundary value problem, the equilibrium equations are solved in the weak form, which is written here as

$$g = \bar{g}(\mathbf{u}, \boldsymbol{\eta}) = \hat{g}(\mathbf{E}, \delta\mathbf{E}) = \int_{\mathcal{B}_0} (\boldsymbol{\tau}_{EQ} + \boldsymbol{\tau}_{NEQ}) : (\mathbf{F}^{-T} \cdot \delta\mathbf{E} \cdot \mathbf{F}^{-1}) \, dV - g_a = 0, \quad (64)$$

where \mathcal{B}_0 is the reference configuration of the body, dV is the volume element in the reference configuration, \mathbf{u} is the displacement vector, $\boldsymbol{\eta}$ a test function, and g_a a short hand notation for the virtual work of the external loading. A common method to solve this nonlinear equation for \mathbf{u} is by means of a Newton iteration, which requires the linearization of (64). If we linearize about $\mathbf{E} = \mathbf{E}_t$, we obtain

$$g \approx \hat{g}(\mathbf{E}_t, \delta\mathbf{E}) + \left. \frac{\partial g}{\partial \mathbf{E}} \right|_{\mathbf{E}_t} : \Delta\mathbf{E} = 0. \quad (65)$$

The term $\partial g / \partial \mathbf{E} : \Delta\mathbf{E}$ is given by

$$\begin{aligned} \frac{\partial g}{\partial \mathbf{E}} : \Delta\mathbf{E} &= \int_{\mathcal{B}_0} \left(\mathbf{F} \cdot \left(\left(\frac{\partial \mathbf{S}_{EQ}}{\partial \mathbf{E}} + \frac{\partial \mathbf{S}_{NEQ}}{\partial \mathbf{E}} \right) : \Delta\mathbf{E} \right) \cdot \mathbf{F}^T \right) : (\mathbf{F}^{-T} \cdot \delta\mathbf{E} \cdot \mathbf{F}^{-1}) \, dV \\ &\quad + \int_{\mathcal{B}_0} (\boldsymbol{\tau}_{EQ} + \boldsymbol{\tau}_{NEQ}) : (\mathbf{F}^{-T} \cdot \Delta\delta\mathbf{E} \cdot \mathbf{F}^{-1}) \, dV \end{aligned} \quad (66)$$

$$\begin{aligned} &= \int_{\mathcal{B}_0} (\mathcal{C}_{EQ} + \mathcal{C}_{NEQ}) : (\mathbf{F}^{-T} \cdot \Delta\mathbf{E} \cdot \mathbf{F}^{-1}) : (\mathbf{F}^{-T} \cdot \delta\mathbf{E} \cdot \mathbf{F}^{-1}) \, dV \\ &\quad + \int_{\mathcal{B}_0} (\boldsymbol{\tau}_{EQ} + \boldsymbol{\tau}_{NEQ}) : (\mathbf{F}^{-T} \cdot \Delta\delta\mathbf{E} \cdot \mathbf{F}^{-1}) \, dV \end{aligned} \quad (67)$$

with

$$\Delta\delta\mathbf{E} = \frac{1}{2}(\Delta\mathbf{F}^T \cdot \delta\mathbf{F} + \delta\mathbf{F}^T \cdot \Delta\mathbf{F}). \quad (68)$$

The second integral in (67) represents the geometric tangent and can be immediately calculated, if the stresses are known. It remains to derive the fourth order constitutive tensors \mathcal{C}_{EQ} and \mathcal{C}_{NEQ} , which are obtained by a push forward transformation of the material tensors

$$\mathcal{L}_{EQ} = \frac{\partial \mathbf{S}_{EQ}}{\partial \mathbf{E}} = \frac{\partial^2 \Psi_{EQ}}{\partial \mathbf{E} \partial \mathbf{E}} \quad (69)$$

and

$$\mathcal{L}_{NEQ} = \frac{\partial \mathbf{S}_{NEQ}}{\partial \mathbf{E}}, \quad (70)$$

to the current configuration. As already discussed, the equilibrium part of the material model is identical with a material model for finite elasticity. Thus, the material tensors, \mathcal{L}_{EQ} or \mathcal{C}_{EQ} , are exactly the same as in finite elasticity. For the derivation of the stress tensor $\boldsymbol{\tau}_{EQ}$ and the material tensors \mathcal{L}_{EQ} and \mathcal{C}_{EQ} based on an Ogden model, see Simo and Taylor (1991) or Reese and Wriggers (1995). The calculation for \mathcal{L}_{NEQ} is new and will be discussed in detail in the following.

Instead of the multiplicative decomposition of \mathbf{F} into $\mathbf{F}_e \cdot \mathbf{F}_i$, we can use the equivalent alternative multiplicative decomposition

$$\mathbf{F} = (\mathbf{F}_e)_{\text{trial}} \cdot (\mathbf{F}_i)_{t=t_{n-1}}, \quad (71)$$

which follows immediately from the fact that $(\mathbf{F}_e)_{\text{trial}} = (\mathbf{F})_{t=t_n} \cdot (\mathbf{F}_i)_{t=t_{n-1}}^{-1}$. The advantage of expression (71) is, that, since $(\mathbf{F}_i)_{t=t_{n-1}}$ has to be treated as a constant at time $t = t_n$, the increment

$$\Delta \mathbf{F} = \Delta(\mathbf{F}_e)_{\text{trial}} \cdot (\mathbf{F}_i)_{t=t_{n-1}} \quad (72)$$

depends only on the increment $(\Delta \mathbf{F}_e)_{\text{trial}}$. This motivates the introduction of a stress tensor $\tilde{\mathbf{S}}_{NEQ}$ defined by

$$\mathbf{S}_{NEQ} = \mathbf{F}^{-1} \cdot \boldsymbol{\tau}_{NEQ} \cdot \mathbf{F}^{-T} = (\mathbf{F}_i)_{t=t_{n-1}}^{-1} \cdot \underbrace{(\mathbf{F}_e)_{\text{trial}}^{-1} \cdot \boldsymbol{\tau}_{NEQ} \cdot (\mathbf{F}_e)_{\text{trial}}^{-T}}_{\tilde{\mathbf{S}}_{NEQ}} \cdot (\mathbf{F}_i)_{t=t_{n-1}}^{-T}. \quad (73)$$

Instead of calculating \mathcal{C}_{NEQ} by computing \mathcal{L}_{NEQ} and carrying out the push-forward with \mathbf{F} , we determine the material tensor

$$\tilde{\mathcal{L}}_{NEQ} = 2 \frac{\partial \tilde{\mathbf{S}}_{NEQ}}{\partial (\mathbf{C}_e)_{\text{trial}}} \quad (74)$$

and then push forward with $(\mathbf{F}_e)_{\text{trial}}$. Based on the spectral decomposition

$$\tilde{\mathbf{S}}_{NEQ} = \sum_{A=1}^3 \frac{\tau_A}{\underbrace{(\lambda_{Ae})^2_{\text{trial}}}_{\tilde{S}_A}} \tilde{\mathbf{N}}_A \otimes \tilde{\mathbf{N}}_A, \quad (75)$$

the derivative of $\tilde{\mathbf{S}}_{NEQ}$ with respect to $(\mathbf{C}_e)_{\text{trial}}$ is derived from

$$\begin{aligned} 2 \frac{\partial \tilde{\mathbf{S}}_{NEQ}}{\partial (\mathbf{C}_e)_{\text{trial}}} : \frac{1}{2} \Delta(\mathbf{C}_e)_{\text{trial}} &= 2 \sum_{B=1}^3 \frac{\partial \tilde{\mathbf{S}}_{NEQ}}{\partial (\varepsilon_{Be})_{\text{trial}}} \otimes \frac{\partial (\varepsilon_{Be})_{\text{trial}}}{\partial (\mathbf{C}_e)_{\text{trial}}} : \frac{1}{2} \Delta(\mathbf{C}_e)_{\text{trial}} \\ &= 2 \sum_{A=1}^3 \sum_{B=1}^3 \frac{\partial \tilde{S}_A}{\partial (\varepsilon_{Be})_{\text{trial}}} \tilde{\mathbf{N}}_A \otimes \tilde{\mathbf{N}}_A \otimes \frac{\partial (\varepsilon_{Be})_{\text{trial}}}{\partial (\mathbf{C}_e)_{\text{trial}}} : \frac{1}{2} \Delta(\mathbf{C}_e)_{\text{trial}} \\ &\quad + \sum_{A=1}^3 \tilde{S}_A \Delta(\tilde{\mathbf{N}}_A \otimes \tilde{\mathbf{N}}_A) \\ &= \Delta \tilde{\mathbf{S}}_{NEQ} = \tilde{\mathcal{L}}_{NEQ} : \frac{1}{2} \Delta(\mathbf{C}_e)_{\text{trial}}. \end{aligned} \quad (76)$$

Interestingly, we can proceed here in the same way as in elastoplasticity. The calculation of $\tilde{\mathcal{L}}_{NEQ}$ consists mainly of the computation of the partial derivatives

$$\frac{\partial \tilde{S}_A}{\partial (\varepsilon_{Be})_{\text{trial}}} \quad \text{and} \quad \frac{\partial (\varepsilon_{Be})_{\text{trial}}}{\partial (\mathbf{C}_e)_{\text{trial}}}. \quad (77)$$

For (77a), we have

$$\frac{\partial \tilde{S}_A}{\partial (\varepsilon_{Be})_{\text{trial}}} = \frac{1}{(\lambda_{Ae})_{\text{trial}}^4} \left(\underbrace{\frac{\partial \tau_A}{\partial (\varepsilon_{Be})_{\text{trial}}}}_{C_{AB}^{\text{alg}}} (\lambda_{Ae})_{\text{trial}}^2 - \tau_A 2 (\lambda_{Ae})_{\text{trial}} \underbrace{\frac{\partial (\lambda_{Ae})_{\text{trial}}}{\partial (\varepsilon_{Be})_{\text{trial}}}}_{(\lambda_{Ae})_{\text{trial}} \delta_{AB}} \right), \quad (78)$$

where the modulus C_{AB}^{alg} , which determines the incremental constitutive relation

$$\Delta \tau_A = \sum_{B=1}^3 C_{AB}^{\text{alg}} \Delta (\varepsilon_{Be})_{\text{trial}}, \quad (79)$$

has to be computed. For the purpose of deriving C_{AB}^{alg} , the condition

$$\Delta r_A = 0 \quad (80)$$

is used. By means of this condition we take into account that the nonlinear equation $r_A = 0$ (see Table 1) is satisfied during every global Newton iteration. Considering the fact that $(\varepsilon_{Ae})_{\text{trial}}$ is not a constant in the global iteration, we obtain

$$\Delta r_A = \sum_{B=1}^3 K_{AB} \Delta \varepsilon_{Be} - \Delta (\varepsilon_{Ae})_{\text{trial}} = 0, \quad (81)$$

from which follows

$$\Delta \tau_A = \sum_{B=1}^3 \frac{\partial \tau_A}{\partial \varepsilon_{Be}} \Delta \varepsilon_{Be} = \sum_{C=1}^3 \underbrace{\sum_{B=1}^3 \frac{\partial \tau_A}{\partial \varepsilon_{Be}} K_{BC}^{-1}}_{C_{AC}^{\text{alg}}} \Delta (\varepsilon_{Ce})_{\text{trial}}. \quad (82)$$

Due to the fact that the evolution eqn (21) arises from a potential [see (38) and Appendix C], the algorithmic tangent modulus C_{AB}^{alg} is symmetric as in associative elastoplasticity. The proof for this important property is given in Appendix C.

The partial derivative $\partial (\varepsilon_{Be})_{\text{trial}} / \partial (\mathbf{C}_e)_{\text{trial}}$ is given by

$$\begin{aligned} \frac{\partial (\mathbf{C}_e)_{\text{trial}}}{\partial (\varepsilon_{Be})_{\text{trial}}} &= \sum_{A=1}^3 \frac{\partial (\lambda_{Ae})_{\text{trial}}^2}{\partial (\varepsilon_{Be})_{\text{trial}}} \tilde{\mathbf{N}}_A \otimes \tilde{\mathbf{N}}_A = \sum_{A=1}^3 2 (\lambda_{Ae})_{\text{trial}} \delta_{AB} (\lambda_{Be})_{\text{trial}} \tilde{\mathbf{N}}_A \otimes \tilde{\mathbf{N}}_A \\ &= 2 (\lambda_{Be})_{\text{trial}}^2 \tilde{\mathbf{N}}_B \otimes \tilde{\mathbf{N}}_B, \end{aligned} \quad (83)$$

which yields

$$2 \frac{\partial (\varepsilon_{Be})_{\text{trial}}}{\partial (\mathbf{C}_e)_{\text{trial}}} = \frac{1}{(\lambda_{Be})_{\text{trial}}^2} \tilde{\mathbf{N}}_B \otimes \tilde{\mathbf{N}}_B. \quad (84)$$

Finally, using the expressions (76), (78) and (84), we obtain for $\Delta \tilde{\mathbf{S}}_{NEQ}$ the relation

$$\begin{aligned} \Delta \tilde{\mathbf{S}}_{NEQ} &= \frac{1}{2} \left(\sum_{A=1}^3 \sum_{B=1}^3 \frac{1}{(\lambda_{Ae})_{\text{trial}}^2 (\lambda_{Be})_{\text{trial}}^2} (C_{AB}^{\text{alg}} - \tau_A 2 \delta_{AB}) \tilde{\mathbf{N}}_A \otimes \tilde{\mathbf{N}}_A \otimes \tilde{\mathbf{N}}_B \otimes \tilde{\mathbf{N}}_B \right) \\ &\quad + 2 \sum_{C=1}^3 ((\lambda_{Ce})_{\text{trial}} \Delta (\lambda_{Ce})_{\text{trial}} \tilde{\mathbf{N}}_C \otimes \tilde{\mathbf{N}}_C) + \sum_{A=1}^3 \tilde{S}_A \Delta (\tilde{\mathbf{N}}_A \otimes \tilde{\mathbf{N}}_A). \end{aligned} \quad (85)$$

Making use of the spin tensor as in Ogden (1984, Section 2.3.2), the stress increment $\Delta \tilde{\mathbf{S}}_{NEQ}$ is given by

$$\Delta \tilde{\mathbf{S}}_{NEQ} = \sum_{A=1}^3 \Delta \tilde{\mathbf{S}}_A \tilde{\mathbf{N}}_A \otimes \tilde{\mathbf{N}}_A + \sum_{A=1}^3 \sum_{B \neq A=1}^3 (\tilde{\mathbf{S}}_B - \tilde{\mathbf{S}}_A) \Omega_{BA} \tilde{\mathbf{N}}_A \otimes \tilde{\mathbf{N}}_B, \quad (86)$$

where Ω_{BA} can be defined through

$$\Delta \tilde{\mathbf{N}}_B = \sum_{C=1}^3 \underbrace{(\tilde{\mathbf{N}}_C \cdot \Delta \tilde{\mathbf{N}}_B)}_{\Omega_{CB}} \tilde{\mathbf{N}}_C. \quad (87)$$

Analogously, we have for the strain increment $(\Delta \mathbf{C}_e)_{\text{trial}}$ the relation

$$\begin{aligned} \frac{1}{2} \Delta (\mathbf{C}_e)_{\text{trial}} = & \frac{1}{2} \left(\sum_{A=1}^3 2(\lambda_{Ae})_{\text{trial}} \Delta (\lambda_{Ae})_{\text{trial}} \tilde{\mathbf{N}}_A \otimes \tilde{\mathbf{N}}_A \right. \\ & \left. + \sum_{A=1}^3 \sum_{B \neq A=1}^3 ((\lambda_{Be})_{\text{trial}}^2 - (\lambda_{Ae})_{\text{trial}}^2) \Omega_{BA} \tilde{\mathbf{N}}_A \otimes \tilde{\mathbf{N}}_B \right). \end{aligned} \quad (88)$$

Taking into account

$$\Delta \tilde{\mathbf{S}}_{NEQ} = \tilde{\mathcal{L}}_{NEQ} : \frac{1}{2} \Delta (\mathbf{C}_e)_{\text{trial}} \quad (89)$$

leads us to the constitutive tensor

$$\begin{aligned} \tilde{\mathcal{L}}_{NEQ} = & \sum_{A=1}^3 \sum_{B=1}^3 \left(\frac{1}{(\lambda_{Ae})_{\text{trial}}^2 (\lambda_{Be})_{\text{trial}}^2} (C_{AB}^{\text{alg}} - \tau_A 2\delta_{AB}) \tilde{\mathbf{N}}_A \otimes \tilde{\mathbf{N}}_A \otimes \tilde{\mathbf{N}}_B \otimes \tilde{\mathbf{N}}_B \right) \\ & + \frac{1}{2} \sum_{A=1}^3 \sum_{B=1}^3 2 \frac{\tilde{\mathbf{S}}_B - \tilde{\mathbf{S}}_A}{(\lambda_{Be})_{\text{trial}}^2 - (\lambda_{Ae})_{\text{trial}}^2} (\tilde{\mathbf{N}}_A \otimes \tilde{\mathbf{N}}_B \otimes \tilde{\mathbf{N}}_A \otimes \tilde{\mathbf{N}}_B \\ & + \tilde{\mathbf{N}}_A \otimes \tilde{\mathbf{N}}_B \otimes \tilde{\mathbf{N}}_B \otimes \tilde{\mathbf{N}}_A) \\ = & \sum_{A=1}^3 \sum_{B=1}^3 \sum_{C=1}^3 \sum_{D=1}^3 \tilde{L}_{ABCD} \tilde{\mathbf{N}}_A \otimes \tilde{\mathbf{N}}_B \otimes \tilde{\mathbf{N}}_C \otimes \tilde{\mathbf{N}}_D, \end{aligned} \quad (90)$$

which finally after the push forward with $(\mathbf{F}_e)_{\text{trial}}$ yields

$$\mathcal{L}_{NEQ} = \sum_{A=1}^3 \sum_{B=1}^3 \sum_{C=1}^3 \sum_{D=1}^3 \underbrace{\tilde{L}_{ABCD} (\lambda_{Ae})_{\text{trial}} (\lambda_{Be})_{\text{trial}} (\lambda_{Ce})_{\text{trial}} (\lambda_{De})_{\text{trial}}}_{C_{ABCD}} \mathbf{n}_A \otimes \mathbf{n}_B \otimes \mathbf{n}_C \otimes \mathbf{n}_D. \quad (91)$$

Note, the material tensor for the equilibrium part of the constitutive model, \mathcal{L}_{EQ} , can be represented in a similar form. The only differences lie in the structure of C_{AB}^{alg} and in the calculation of the shear terms C_{1212} , C_{2323} and C_{3131} . Additionally, in the NEQ-case the elastic principal trial stretches $(\lambda_{Ae})_{\text{trial}}$ are used instead of λ_A . The symmetry $C_{ABCD} = C_{CDAB}$ of the material tensor \mathcal{L}_{NEQ} is given through the symmetry of the algorithmic tangent modulus C_{AB}^{alg} .

5. EXAMPLES

For the calculations shown below the material model was fit to experimental results¹ for a vulcanized natural rubber. We obtained the following material parameters:

¹ Unpublished.

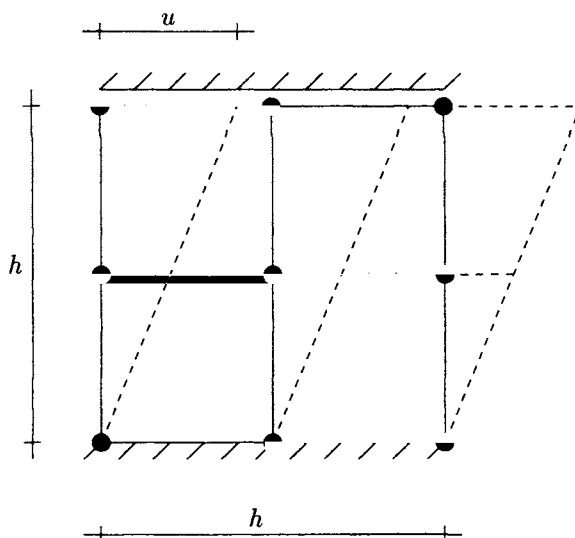


Fig. 2. Shear test geometry and discretization; all boundary nodes are driven.

$$\begin{aligned}
 \mu_1 &= 20 \text{ psi}; & \alpha_1 &= 1.8 \\
 \mu_2 &= -7 \text{ psi}; & \alpha_2 &= -2 \\
 \mu_3 &= 1.5 \text{ psi}; & \alpha_3 &= 7 \\
 (\mu_m)_1 &= 51.4 \text{ psi}; & (\alpha_m)_1 &= 1.8 \\
 (\mu_m)_2 &= -18 \text{ psi}; & (\alpha_m)_2 &= -2 \\
 (\mu_m)_3 &= 3.86 \text{ psi}; & (\alpha_m)_3 &= 7. \\
 \tau &= 17.5 \text{ s}
 \end{aligned} \tag{92}$$

In order to simplify the fit, we chose for all three pairs ($r = 1, 2, 3$) the same factor $(\mu_m)_r/\mu_r$. Moreover, the same exponents $(\alpha_r = (\alpha_m)_r)$ were used for the equilibrium and the non-equilibrium parts of the material model.

To avoid volumetric locking effects, the finite element calculations were carried out by means of a mixed formulation according to Sussman and Bathe (1987), which requires the computation of a so-called mixed pressure for each element. It is numerically convenient to calculate the pressure outside of the main Gauss point loop. For this purpose, we neglected the volumetric part of the evolution equation in the numerical calculations shown below. It has to be emphasized that the only reason for this was a higher computational efficiency. All finite element calculations were carried out using the finite element program FEAP (developed at UC Berkeley by Professor R. L. Taylor and partially documented in Zienkiewicz and Taylor, 1989, 1991). We will use the shorthand notation FLV for the theory of finite linear viscoelasticity based on the evolution (31) and FV for the theory of finite viscoelasticity based on (21). For all examples a plane strain state was assumed.

5.1. Shear test with sinusoidal loading

In Fig. 3(a–d) the Cauchy shear stress is plotted vs the engineering shear strain $u/h \cdot 100\%$ for four different amplitudes u_0 of the sinusoidal loading $u = u_0 \sin \omega t$ (see Fig. 2). The frequency was chosen to be 0.3 s^{-1} . The maximal shear strains were 1% (Fig. 3(a)), 100% (Fig. 3(b)), 200% (Fig. 3(c)) and 500% (Fig. 3(d)). In Fig. 4(a–b) the shear component $(b_e)_{12}$ of $\mathbf{b}_e = \sum_{i=1}^3 \sum_{j=1}^3 (b_e)_{ij} \mathbf{e}_i \otimes \mathbf{e}_j$ (\mathbf{e}_i Cartesian unit vectors) is shown as a function of the time t for each of these numerical simulations. For every test five loading cycles were calculated. As expected for only 1% maximal shear strain the curves for FV and FLV (Fig. 3(a)) are identical. At 100% shear strain, however, it can be seen that for

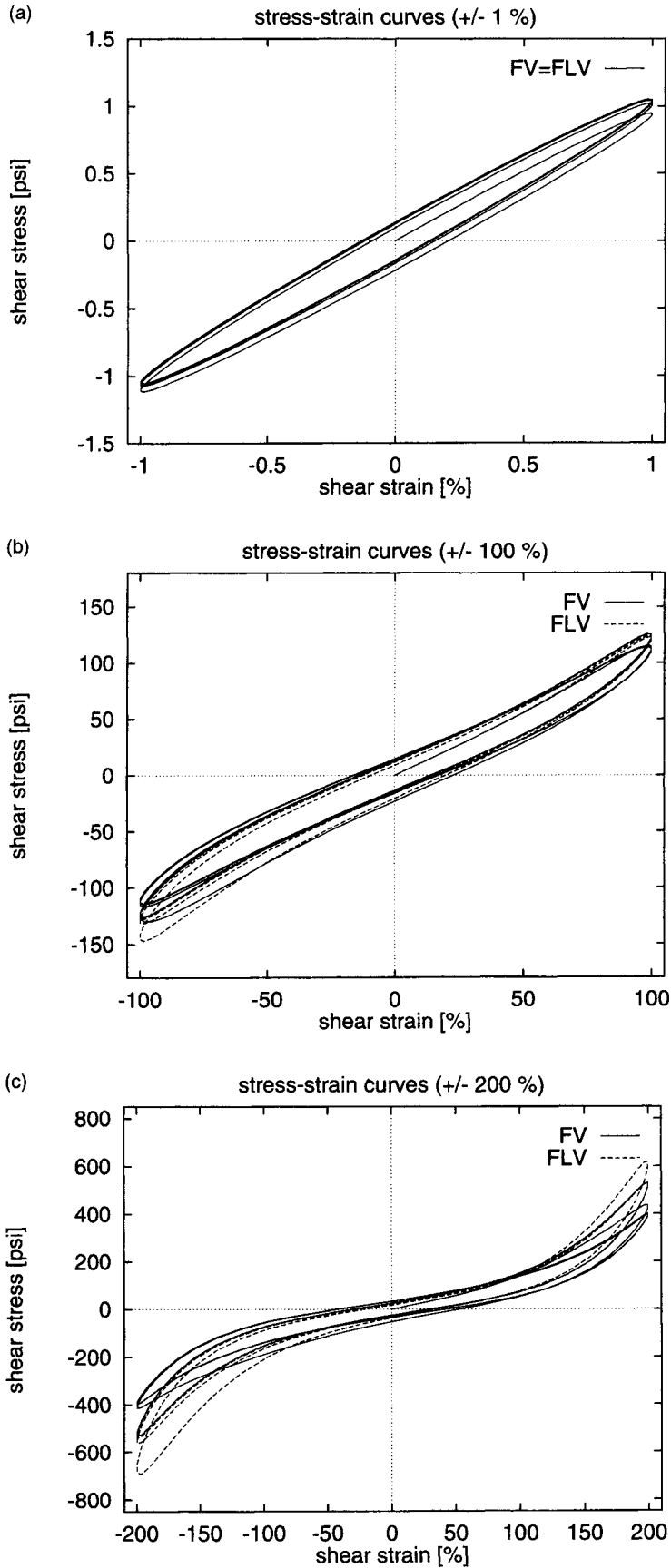


Fig. 3. Shear test : stress-strain curves for $\omega = 0.3 \text{ s}^{-1}$ at a maximum shear strain of (a) $\pm 1\%$, (b) $\pm 100\%$, (c) $\pm 200\%$ and (d) $\pm 500\%$.

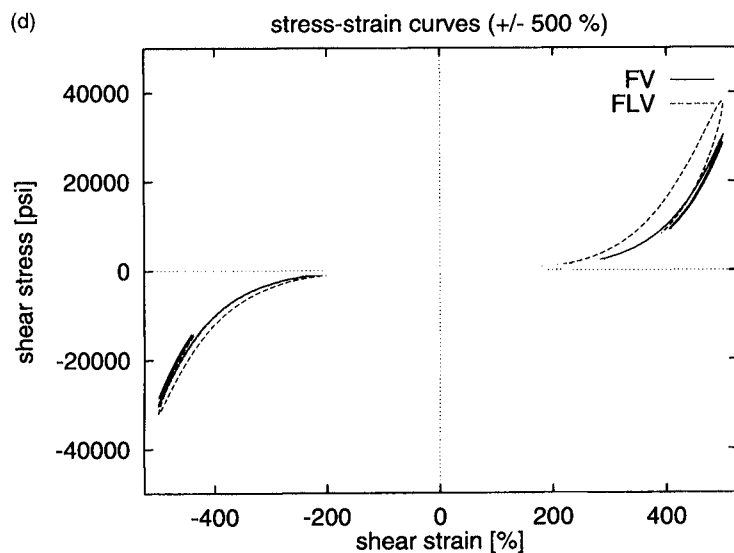


Fig. 3. (continued).

FLV more cycles are needed to obtain the so-called dynamic equilibrium state. Considering Fig. 4(a–b) the difference between the dynamic equilibrium state and the thermodynamic equilibrium state is immediately clear: in the dynamic equilibrium state we have periodic oscillations around the thermodynamic equilibrium state $\mathbf{b}_e = \mathbf{1} \Rightarrow (b_e)_{12} = 0$. Due to the fact that FLV always gives higher values for $(b_e)_{12}$ than FV, using the simplified theory of FLV means one also overestimates the stresses. Interestingly, the shape of the curves in Fig. 4(a) (FV) loses for large maximal strains its sinusoidal form, whereas the curves for FLV maintain it. This can be explained by the fact that for FLV we have a linear relationship between $\dot{\mathbf{C}}_i$ and $\mathbf{C} - \mathbf{C}_i$ [see eqn (37)]. If \mathbf{u} has a sinusoidal form, the special form of (37) or (31), respectively, forces \mathbf{C}_i or \mathbf{b}_e to be also sinusoidal. This behaviour is independent of the size of the maximum strain and shows the linearity, which is hidden in this kind of theory. Furthermore, it is interesting that for FLV the “elastic” shear strain $(b_e)_{12}$ increases with increasing maximum shear strain, whereas for FV we have for 100, 200 and 500% about the same values. We can discuss now also the size of the deviations away from thermodynamic equilibrium. At 100% maximum shear strain we find $\max(b_e)_{12} = 0.8 \cong 80\%$. In thermodynamic equilibrium $[(b_e)_{12}]_{EQ} = 0$ holds. Thus, already for a moderate shear strain of 100% the value of $(b_e)_{12}$ is far from thermodynamic equilibrium. Whether a theory of finite linear viscoelasticity is still realistic in this range of deformation is then questionable. Another interesting issue is how large can the time step Δt be chosen. Figure 5(a,b) shows a convergence study for $\omega = 0.3 \text{ s}^{-1}$ at a maximum shear strain of 200%. One cycle was calculated for FV and FLV with a different number of time steps. Already with 16 steps one obtains especially for FV a quite good solution, which shows the excellent convergence properties of the exponential time integration algorithm.

5.2. Creep problem

As a second simple example we consider a creep problem. This example has already been dealt with by Holzapfel (1996). The material parameters for this example were

$$\mu_1 = 0.63 \text{ N/mm}^2; \quad \alpha_1 = 1.3$$

$$\mu_2 = -0.01 \text{ N/mm}^2; \quad \alpha_2 = -2$$

$$\mu_3 = 0.0012 \text{ N/mm}^2; \quad \alpha_1 = 5$$

$$(\mu_m)_1 = 0.63 \text{ N/mm}^2; \quad (\alpha_m)_1 = 1.3$$

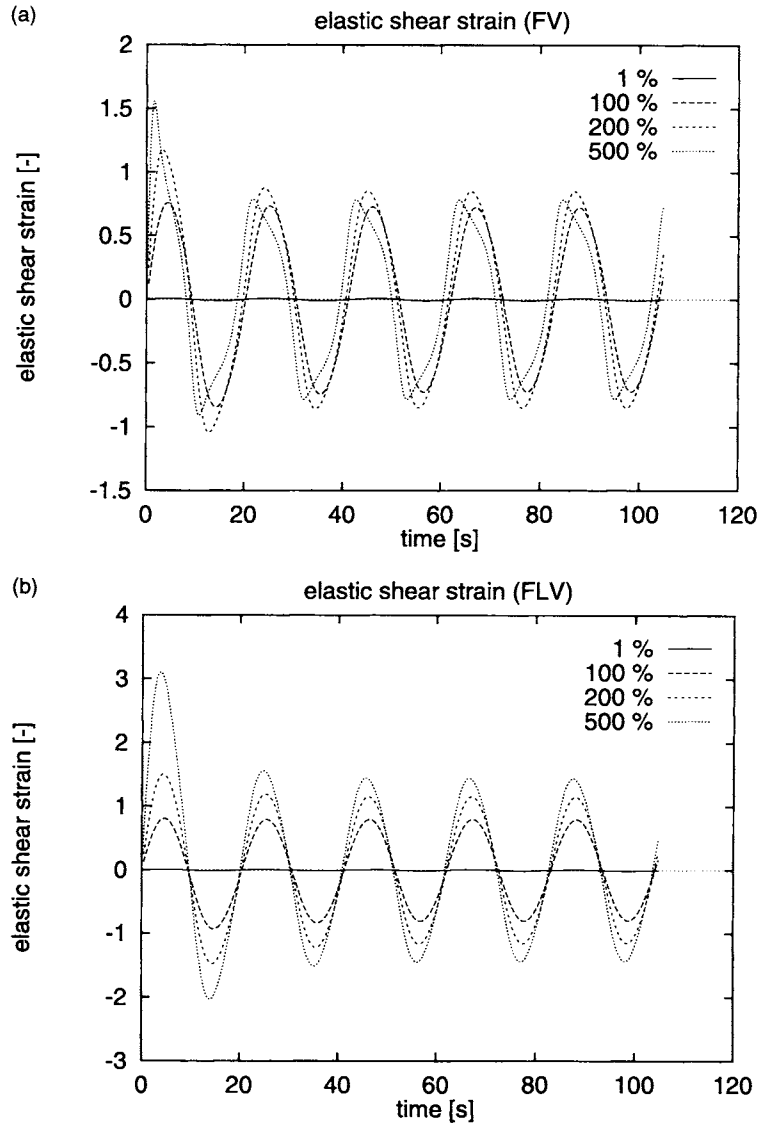


Fig. 4. Shear test: “elastic” shear strain $(b_e)_{12}$ as a function of the time for different maximum strains: (a) finite viscoelasticity; (b) finite linear viscoelasticity.

$$\begin{aligned}
 (\mu_m)_2 &= -0.1 \text{ N/mm}^2; & (\alpha_m)_2 &= -2 \\
 (\mu_m)_3 &= 0.0012 \text{ N/mm}^2; & (\alpha_m)_3 &= 5 \\
 \tau_1 &= 30 \text{ s}; & \tau_2 &= 20 \text{ s}; & K &= 2000 \text{ N/mm}^2.
 \end{aligned} \tag{93}$$

Note that the model of Holzapfel (1996) is based on the assumption

$$\Psi_{NEQ} = \beta \Psi_{EQ},$$

the constant factor β being an additional material parameter. For the example at hand it was chosen to be one. Since in our case Ψ_{NEQ} depends on the elastic principal stretches λ_{Ae} instead of λ_A as in Holzapfel’s model, the numerical results would not be comparable. To take this into account, we chose a different second relaxation time ($\tau_2 = 10$ s). The geometry of the system and the boundary and loading conditions are described in Fig. 6. For this example we used an isoparametric 3D displacement element formulation. The calculation

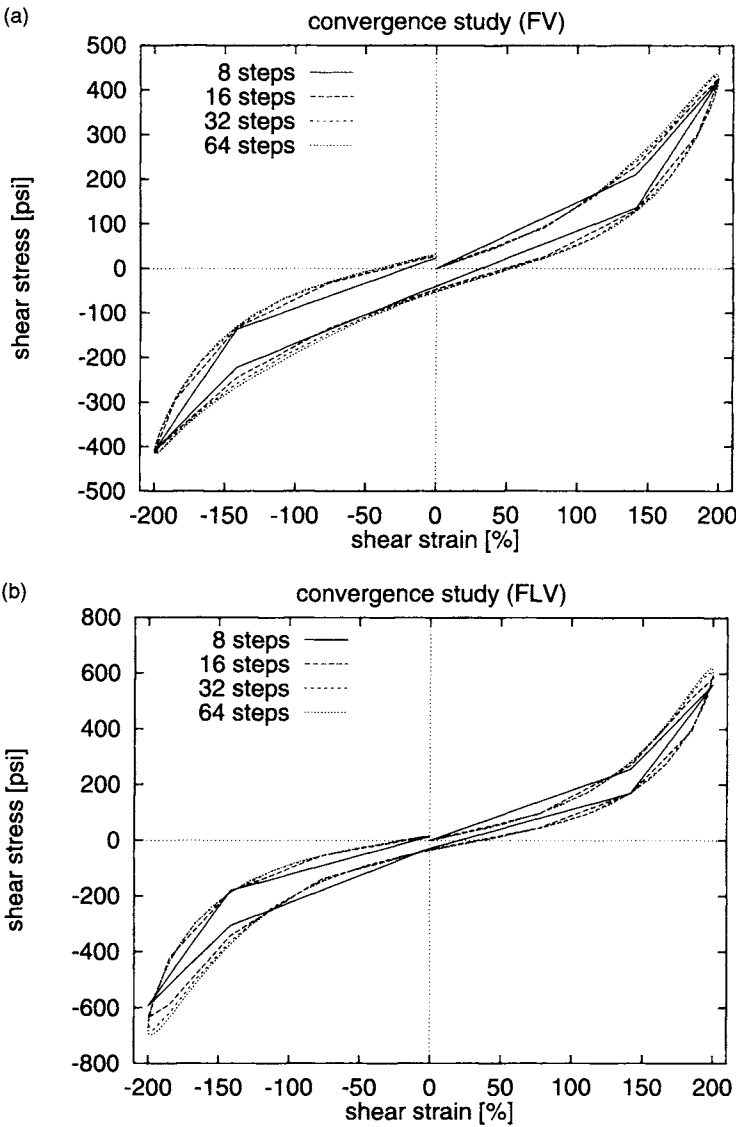


Fig. 5. Convergence study : single stress–strain loops with varying time step sizes : (a) FV ; (b) FLV.

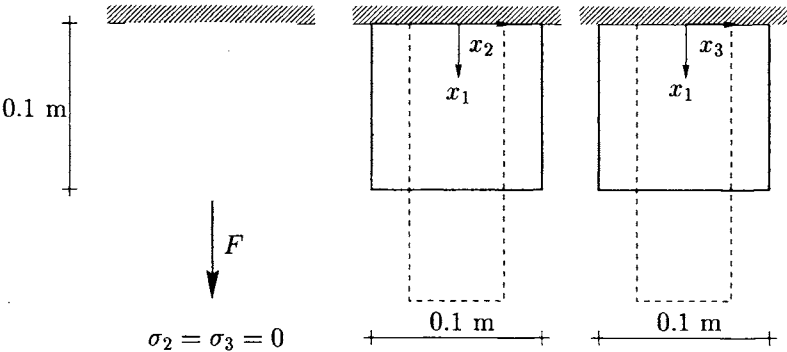


Fig. 6. Creep problem : geometry and loading.

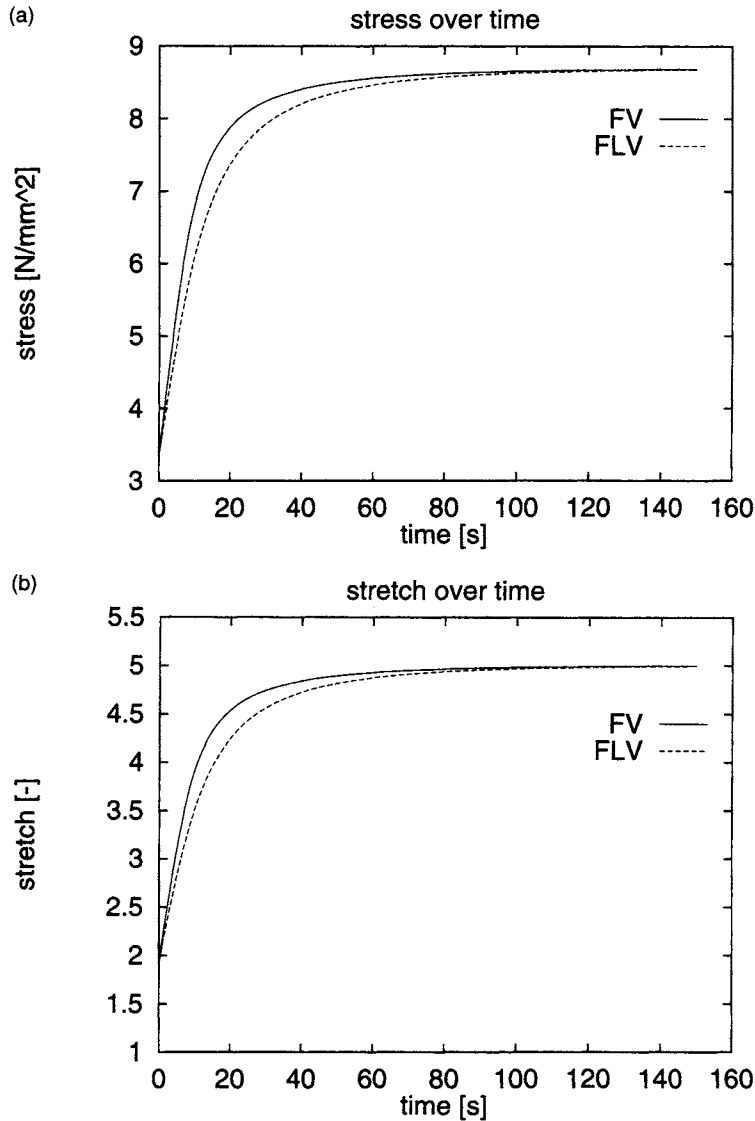


Fig. 7. Creep problem : stress and stretch in load direction as a function of time : (a) stress σ_{11} ; (b) stretch λ_1 .

was performed with only one element, representing one quarter of the system depicted in Fig. 6. The load (1085.625 N at each node) was applied on one step ($t = 0$ s) and then held constant. We chose the following time steps: $0 \text{ s} < t < 5 \text{ s}$: $\Delta t = 0.25 \text{ s}$, $5 \text{ s} < t < 15 \text{ s}$: $\Delta t = 0.5 \text{ s}$, $15 \text{ s} < t < 150 \text{ s}$: $\Delta t = 1 \text{ s}$. The results for FLV and FV are shown in Fig. 7. As expected, the results for FLV agree with the ones of Holzapfel (1996), since his model is derived from a theory of finite linear viscoelasticity. The results for FV, however, show that using FV one obtains a faster approach to thermodynamic equilibrium.

A comparison of some quantitative results is also given in Table 2 below.

5.3. Bearing

We finally show the applicability of the derived theory of finite viscoelasticity in a quite practical and general example, the shearing of a rubber–steel bearing. Bearings of the type shown are used as base isolation against earthquake loading. The discretization of the bearing and the boundary conditions are given in Fig. 8. The material parameters for the rubber are as in (92), i.e.

Table 2. Stretch values obtained with different material models

Time	Holzapfel (1996)	FLV	FV
0 s	1.93	1.93	1.93
5 s	2.84	2.82	3.11
15 s	3.95	3.96	4.33
$t \rightarrow \infty$	$\lambda \rightarrow 5$	$\lambda \rightarrow 5$	$\lambda \rightarrow 5$

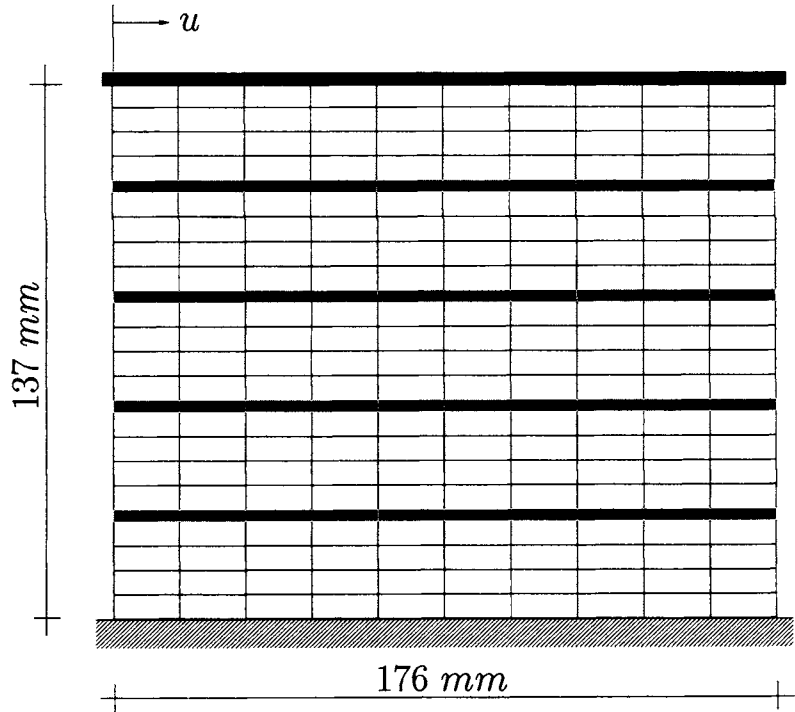


Fig. 8. Bearing geometry and loading : dark elements are steel (one steel layer 3 mm) ; light elements rubber (one rubber layer 25 mm) ; top plate rigid.

$$\begin{aligned} \mu_1 &= 0.1379 \text{ N/mm}^2 ; \quad \alpha_1 = 1.8 \\ \mu_2 &= -0.04827 \text{ N/mm}^2 ; \quad \alpha_2 = -2 \\ \mu_3 &= 0.01034 \text{ N/mm}^2 ; \quad \alpha_1 = 7 \\ (\mu_m)_1 &= 0.3544 \text{ N/mm}^2 ; \quad (\alpha_m)_1 = 1.8 \\ (\mu_m)_2 &= -0.124 \text{ N/mm}^2 ; \quad (\alpha_m)_2 = -2 \\ (\mu_m)_3 &= 0.0266 \text{ N/mm}^2 ; \quad (\alpha_m)_3 = 7 \\ \tau &= 17.5 \text{ s.} \end{aligned} \tag{94}$$

For steel we have

$$\begin{aligned} (\mu_1)_{St} &= 80,769.231 \text{ N/mm}^2 ; \quad (\alpha_1)_{St} = 2.0 \\ (K)_{St} &= 121,153.85 \text{ N/mm}^2. \end{aligned} \tag{95}$$

The nodes of the upper rubber layer are linked together such that they have the same

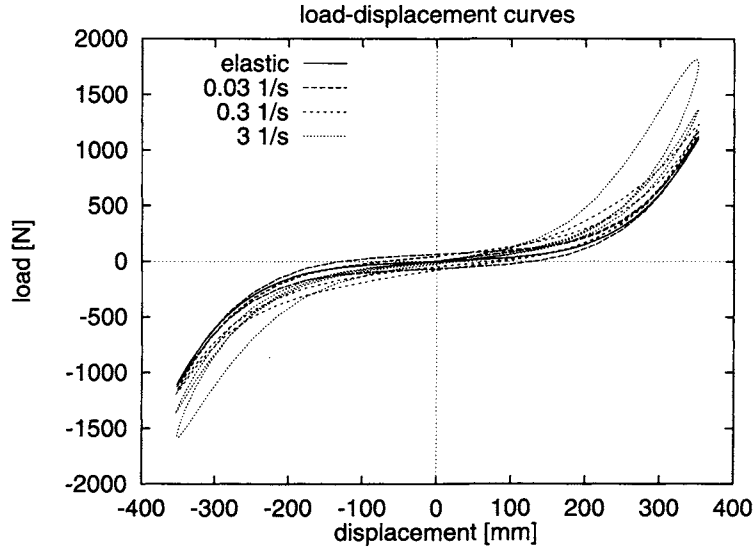


Fig. 9. Load–displacement curves at top of bearing for different frequencies in finite viscoelasticity.

displacement in the y -direction. The loading was a sinusoidal horizontal displacement of the upper layer for three different frequencies.

In Fig. 9, the reaction force in the x -direction in the upper layer is plotted vs the displacement in the same direction. For this calculation the loading was applied in sinusoidal form. At each frequency two cycles were calculated. At higher frequencies more cycles are needed to obtain dynamic equilibrium. This is due to the fact that the necessary time for the system to obtain the dynamic equilibrium state is mainly determined by the relaxation time. Thus, for a higher frequency more cycles fit in this “pre-equilibrium” time period. For a very low frequency, rate-dependent effects play a negligible role and we come to the same results as with an ideally elastic Ogden model using the material parameters for the equilibrium part. The latter calculations were carried out with $K = 50 \text{ N/mm}^2$.

In a second calculation, the bulk modulus was set to $K = 500 \text{ N/mm}^2$. In Fig. 10(a,b) the system is plotted for two deformed states. The bearing was sheared at a rate of 5% engineering shear strain per s. The time step was chosen to be 1 s, such that 300% shear strain was reached in 60 time steps.

In order to show the convergence behaviour of the global Newton iteration, in Table 3 the norm of the residual force vector in each iteration is plotted for two load steps of different size. As it is characteristic for a consistent linearization, the convergence rate near the solution is independent of the size of the chosen load step.

6. CLOSURE

Many material models in large deformation viscoelasticity are based on linear evolution equations for the internal variable. One goal of this paper was to show that such theories are restricted to states close to thermodynamic equilibrium. Thus, these models are not suitable for systems which suffer large creep deformations. In the present paper, we derive a model of viscoelasticity which accounts for both large deformations and large deviations away from thermodynamic equilibrium. By a linearization procedure about thermodynamic equilibrium, we recover several material models of finite linear viscoelasticity. It is concluded that models of this kind cannot be considered as generally applicable, a fact which has not previously been sufficiently emphasized in the literature.

The presented theory is based on a split of the free energy into an equilibrium part and a non-equilibrium part. Using a multiplicative decomposition of the deformation gradient into elastic and inelastic parts, we developed an algorithm similar to the exponential mapping algorithm in associative elastoplasticity. The implementation of the model for

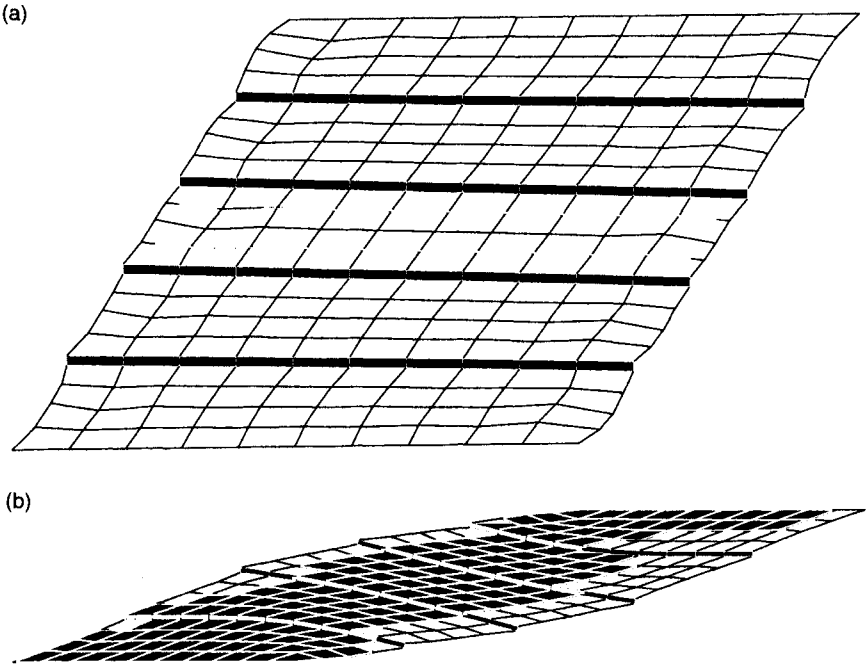


Fig. 10. Deformed bearing at (a) 50% and (b) 200% shear strain.

Table 3. Residual norm

Iteration	$\ G\ $	
	Small step (100 \rightarrow 105% in 1 s)	Small step \times 10 (100 \rightarrow 150% in 10 s)
1	$6.727 \cdot 10^2$	$6.778 \cdot 10^3$
2	$4.957 \cdot 10^1$	$3.901 \cdot 10^3$
3	$1.350 \cdot 10^{-2}$	$3.719 \cdot 10^2$
4	$6.657 \cdot 10^{-7}$	$5.585 \cdot 10^1$
5		$9.708 \cdot 10^1$
6		$3.542 \cdot 10^0$
7		$3.035 \cdot 10^0$
8		$2.042 \cdot 10^{-3}$
9		$2.692 \cdot 10^{-6}$

finite viscoelasticity is as simple as the coding of the linearized model. The only difference lies in the fact that for the general model a non-linear equation has to be solved at the Gauss point level, whereas for the linearized model this equation is linear and can therefore be solved directly.

By means of examples it was shown that finite viscoelasticity begins to deviate significantly from shear strains in a moderate range, e.g. 100%. Using the theory of finite viscoelasticity leads to a faster relaxation to equilibrium and much lower stresses. Another interesting feature are the good convergence properties of the exponential mapping algorithm. The example of the bearing shows that the presented algorithm is also appropriate for more sophisticated applications. The finite element formulation is especially efficient since the weak form of equilibrium is solved by means of the Newton method, which requires the consistent linearization of the global equations. In this way we can solve the highly non-linear equations successfully for very large load steps and even in sophisticated examples like the bearing.

We further note that the material model was easily fitted to experimental results—showing that it is appropriate for modelling realistic material behaviour. In addition, the

more general finite viscoelastic model does not include more material parameters than the finite linear model.

A very important influence on viscoelastic material behaviour is given through the temperature dependence of the material parameters and the relaxation time. Moreover, dissipation effects play an important role. The algorithm presented here was restricted to isothermal processes in order to point out the difference between different theories of viscoelasticity and to motivate the use of a theory of finite viscoelasticity. The incorporation of thermal effects, however, does not represent a major problem in the framework of this theory and will appear in a future work.

Acknowledgment—S. Reese gratefully acknowledges the financial support of the Deutsche Forschungsgemeinschaft (DFG) for a post-doctoral research fellowship at the University of California at Berkeley.

REFERENCES

- Ball, J. M. (1977) Convexity conditions and existence theorems in nonlinear elasticity. *Archive for Rational Mechanics and Analysis* **63**, 337–403.
- Boyce, M. C., Parks, D. M. and Argon, A. S. (1988) Large inelastic deformation of glassy polymers, Part I: rate dependent constitutive model. *Mechanics of Materials* **7**, 15–33.
- Christensen, R. M. (1980) A nonlinear theory of viscoelasticity for application to elastomers. *ASME Journal of Applied Mechanics* **47**, 762–768.
- Coleman, B. D. and Gurtin, M. E. (1967) Thermodynamics with internal state variables. *Journal of Chemical Physics* **47**, 597–613.
- Coleman, B. D. and Noll, W. (1961) Foundations of linear viscoelasticity. *Reviews of Modern Physics* **33**, 239–249.
- Crochet, M. J. and Naghdi, P. M. (1969) A class of simple solids with fading memory. *International Journal of Engineering Science* **7**, 1173–1198.
- Cuitino, A. and Ortiz, M. (1992) A material-independent method for extending stress update algorithms from small-strain plasticity to finite plasticity with multiplicative kinematics. *Engineering Computations* **9**, 437–451.
- Dafalias, Y. F. (1991) Constitutive model for large viscoelastic deformations of elastomeric materials. *Mechanics Research Communications* **18**, 61–66.
- Fung, Y. C. (1994) *A First Course in Continuum Mechanics for Physical and Biological Engineers and Scientists*. Prentice Hall, Englewood Cliffs.
- Govindjee, S. and Reese, S. (1997) A presentation and comparison of two large deformation viscoelasticity models. *ASME Journal of Engineering Materials and Technology* **119**, 251–255.
- Govindjee, S. and Simo, J. C. (1992) Mullins' effect and the strain amplitude dependence of the storage modulus. *International Journal of Solids and Structures* **29**, 1737–1751.
- Govindjee, S. and Simo, J. C. (1993) Coupled stress–diffusion: case II. *Journal of the Mechanics and Physics of Solids* **41**, 863–867.
- Green, M. S. and Tobolsky, A. V. (1946) A new approach to the theory of relaxing polymeric media. *Journal of Chemical Physics* **14**, 80–92.
- Gurtin, M. E. (1981) *An Introduction to Continuum Mechanics*. Academic Press, New York.
- Haupt, P. (1993a) On the mathematical modelling of material behaviour in continuum mechanics. *Acta Mechanica* **100**, 129–154.
- Haupt, P. (1993b) Thermodynamics of solids. In *Non-Equilibrium Thermodynamics with Applications to Solids*, ed. W. Muschik. CISM courses and lectures No. 336. International Centre for Mechanical Sciences, pp. 65–138. Springer, Wien—New York.
- Holzapfel, G. A. (1996) On large strain viscoelasticity: continuum formulation and finite element applications to elastomeric structures. *International Journal for Numerical Methods in Engineering* **39**, 3903–3926.
- James, H. M. and Guth, E. (1943) Theory of the elastic properties of rubber. *Journal of Chemical Physics* **11**, 455–481.
- James, H. M. and Guth, E. (1949) Simple presentation of network theory of rubber, with a discussion of other theories. *Journal of Polymer Science* **4**, 153–182.
- Kaliske, M. and Rothert, H. (1997) Formulation and implementation of three-dimensional viscoelasticity at small and finite strains. *Computational Mechanics* **19**, 238–239.
- Koh, S. L. and Eringen, A. C. (1963) On the foundations of non-linear thermo-viscoelasticity. *International Journal of Engineering Science* **1**, 199–229.
- Le Tallec, P., Rahier, C. and Kaiss, A. (1993) Three-dimensional incompressible viscoelasticity in large strains: formulation and numerical approximation. *Computer Methods in Applied Mechanics and Engineering* **109**, 223–258.
- Lee, E. H. (1969) Elastic–plastic deformation at finite strains. *Journal of Applied Mechanics* **36**, 1–6.
- Lion, A. (1996a) A constitutive model for carbon black filled rubber. Experimental investigations and mathematical representations. *Continuum Mechanics and Thermodynamics* **8**, 153–169.
- Lion, A. (1996b) On the mathematical representation of the thermomechanical behaviour of elastomers, Report-No. 1/1996 of the Institute of Mechanics. University of Kassel, Germany, to appear in *Acta Mechanica*, 1997.
- Lubliner, J. (1985) A model of rubber viscoelasticity. *Mechanics Research Communications* **12**, 93–99.
- Miehe, C. (1994) Aspects of the formulation and finite element implementation of large strain isotropic elasticity. *International Journal of Numerical Methods in Engineering* **37**, 1981–2004.
- Miehe, C. (1995) Entropic thermoelasticity at finite strains. Aspects of the formulation and numerical implementation. *Computer Methods in Applied Mechanics and Engineering* **120**, 243–269.

- Ogden, R. W. (1972a) Large deformation isotropic elasticity: on the correlation of theory and experiment for incompressible rubberlike solids. *Proceedings of the Royal Society of London, Series A* **326**, 565–584.
- Ogden, R. W. (1972b) Large deformation isotropic elasticity: on the correlation of theory and experiment for compressible rubberlike solids. *Proceedings of the Royal Society of London, Series A* **328**, 567–583.
- Ogden, R. W. (1984) *Nonlinear Elastic Deformations*. Ellis Horwood, Chichester.
- Reese, S. and Wriggers, P. (1995) A finite element method for stability problems in finite elasticity. *International Journal for Numerical Methods in Engineering* **38**, 1171–1200.
- Sidoroff, F. (1974) Un modèle viscoélastique non linéaire avec configuration intermédiaire. *Journal de Mécanique* **13**, 679–713.
- Simo, J. C. (1987) On a fully three-dimensional finite-strain viscoelastic damage model: formulation and computational aspects. *Computer Methods in Applied Mechanics and Engineering* **60**, 153–173.
- Simo, J. C. (1992) Algorithms for static and dynamic multiplicative plasticity that preserve the classical return mapping schemes of the infinitesimal theory. *Computer Methods in Applied Mechanics and Engineering* **99**, 61–112.
- Simo, J. C. and Miehe, C. (1992) Associative coupled thermoplasticity at finite strains: formulation, numerical analysis and implementation. *Computer Methods in Applied Mechanics and Engineering* **98**, 41–104.
- Simo, J. C. and Taylor, R. L. (1991) Quasi-incompressible finite elasticity in principal stretches. Continuum basis and numerical algorithms. *Computer Methods in Applied Mechanics and Engineering* **65**, 273–310.
- Sussman, T. and Bathe, K.-J. (1987) A finite element formulation for nonlinear incompressible elastic and inelastic analysis. *Computers and Structures* **26**, 357–409.
- Treloar, L. R. G. (1943a) I: The elasticity of a network of long-chain-molecules. *Transactions of the Faraday Society* **39**, 36–41.
- Treloar, L. R. G. (1943b) II: The elasticity of a network of long-chain-molecules. *Transactions of the Faraday Society* **39**, 241–246.
- Treloar, L. R. G. (1975) *The Physics of Rubber Elasticity*. Clarendon Press, Oxford.
- Tschoegl, N. W. (1989) *The Phenomenological Theory of Linear Viscoelastic Behaviour: An Introduction*. Springer, New York.
- Valanis, K. C. (1966) Thermodynamics of large viscoelastic deformations. *Journal of Mathematics and Physics* **45**, 197–212.
- Weber, G. and Anand, L. (1990) Finite deformation constitutive equations and a time integration procedure for isotropic hyperelastic-viscoplastic solids. *Computer Methods in Applied Mechanics and Engineering* **79**, 173–202.
- Zienkiewicz, O. C. and Taylor, R. L. (1989) *The Finite Element Method, Vol. I: Basis Formulation and Linear Problems*. McGraw-Hill, Maidenhead.
- Zienkiewicz, O. C. and Taylor, R. L. (1991) *The Finite Element Method, Vol. II: Solid and Fluid Mechanics, Dynamics and Non-linearity*. McGraw-Hill, Maidenhead.

APPENDIX A

In this Appendix, we prove the assertion that \mathbf{b} and $(\mathbf{b}_e)_{\text{trial}}$ share the same set of eigenvectors (i.e. eigenspace) in the case of isotropy. Note first that

$$\mathbf{b}_e = \underbrace{\exp[-2\Delta t \mathcal{V}^{-1} : \boldsymbol{\tau}_{NEQ}]}_{\mathbf{a}} \cdot (\mathbf{b}_e)_{\text{trial}}. \quad (\text{A1})$$

By the assumption of isotropy on Ψ_{NEQ} , we have that $\boldsymbol{\tau}_{NEQ}$ has the same eigenspace as \mathbf{b}_e by the well known isotropic tensor function representation theorem; see e.g. Gurtin (1981, Section 37) and references therein. Since \mathcal{V}^{-1} is an isotropic rank four tensor, $\mathcal{V}^{-1} : \boldsymbol{\tau}_{NEQ}$ also shares the same eigenspace as \mathbf{b}_e . Further by the definition of the exponential map, we have that \mathbf{a} has the same eigenspace as \mathbf{b}_e . Since the inverse of \mathbf{a} is guaranteed to exist by the properties of the exponential map on symmetric tensors, we may write

$$\mathbf{a}^{-1} \cdot \mathbf{b}_e = (\mathbf{b}_e)_{\text{trial}}. \quad (\text{A2})$$

Note that $\mathbf{a}^{-1} \cdot \mathbf{b}_e$ and \mathbf{b}_e also share the same eigenspace. Thus, we conclude \mathbf{b}_e and $(\mathbf{b}_e)_{\text{trial}}$ have the same eigenspace and we may solve (A1) in terms of principal values. Note that the result is independent of repeated eigenvalues; \mathbf{b}_e and $(\mathbf{b}_e)_{\text{trial}}$ must always have the same degeneracies.

APPENDIX B

In this Appendix, we describe in detail the calculation for the matrix

$$K_{AB} = \frac{\partial r_A}{\partial \varepsilon_{B_e}}, \quad (\text{B1})$$

where r_A is given by

$$r_A = \varepsilon_{Ae} + \Delta t \left(\frac{1}{2\eta_D} \text{dev } \boldsymbol{\tau}_A + \frac{1}{9\eta_V} \boldsymbol{\tau}_{NEQ} : \mathbf{1} \right) - (\varepsilon_{Ae})_{\text{trial}} = 0. \quad (\text{B2})$$

First the principal stresses

$$\tau_A = \underbrace{\sum_{B=1}^3 \frac{\partial(\Psi_{NEQ})_D}{\partial b_{Be}} \frac{\partial \bar{b}_{Be}}{\partial \lambda_{Ae}} \lambda_{Ae}}_{\text{dev } \tau_A} + \underbrace{\frac{\partial(\Psi_{NEQ})_V}{\partial J_e} J_e}_{\frac{1}{3} \tau_{NEQ} : \mathbf{1}} \quad (\text{B3})$$

have to be determined. The required derivatives are given by

$$\frac{\partial(\Psi_{NEQ})_D}{\partial b_{Be}} = \sum_{r=1}^3 \frac{(\mu_m)_r}{2} \bar{b}_{Ae}^{[(\alpha_m)_r/2]-1}, \quad (\text{B4})$$

$$\frac{\partial(\Psi_{NEQ})_V}{\partial J_e} = \frac{K_m}{2} \left(J_e - \frac{1}{J_e} \right), \quad (\text{B5})$$

$$\frac{\partial \bar{b}_{Ae}}{\partial \lambda_{Ae}} = \frac{4}{3} J_e^{-(2/3)} \lambda_{Ae}, \quad (\text{B6})$$

$$\frac{\partial \bar{b}_{Ae}}{\partial \lambda_{Be}} = -\frac{2}{3} J_e^{-(2/3)} \frac{\lambda_{Ae}^2}{\lambda_{Be}}, \quad (A \neq B). \quad (\text{B7})$$

Thus, one obtains with $A \neq B$, $A \neq C$, $B \neq C$:

$$\begin{aligned} \tau_A = \sum_{r=1}^3 \frac{(\mu_m)_r}{2} \left(\bar{b}_{Ae}^{[(\alpha_m)_r/2]-1} \underbrace{\frac{4}{3} J_e^{-(2/3)} \lambda_{Ae}^2}_{\bar{b}_{Ae}} - \bar{b}_{Be}^{[(\alpha_m)_r/2]-1} \underbrace{\frac{2}{3} J_e^{-(2/3)} \lambda_{Be}^2}_{\bar{b}_{Be}} - \bar{b}_{Ce}^{[(\alpha_m)_r/2]-1} \underbrace{\frac{2}{3} J_e^{-(2/3)} \lambda_{Ce}^2}_{\bar{b}_{Ce}} \right) \\ + \frac{K_m}{2} (J_e^2 - 1) = \underbrace{\sum_{r=1}^3 (\mu_m)_r \left(\frac{2}{3} \bar{b}_{Ae}^{(\alpha_m)_r/2} - \frac{1}{3} \bar{b}_{Be}^{(\alpha_m)_r/2} - \frac{1}{3} \bar{b}_{Ce}^{(\alpha_m)_r/2} \right)}_{\text{dev } \tau_A} + \underbrace{\frac{K_m}{2} (J_e^2 - 1)}_{\frac{1}{3} \tau_{NEQ} : \mathbf{1}}. \quad (\text{B8}) \end{aligned}$$

By means of the relations

$$\frac{\partial \bar{b}_{Ae}}{\partial \varepsilon_{Ae}} = \frac{\partial \bar{b}_{Ae}}{\partial \lambda_{Ae}} \lambda_{Ae} = \frac{4}{3} \bar{b}_{Ae}, \quad (\text{B9})$$

$$\frac{\partial \bar{b}_{Ae}}{\partial \varepsilon_{Be}} = \frac{\partial \bar{b}_{Ae}}{\partial \lambda_{Be}} \lambda_{Be} = -\frac{2}{3} \bar{b}_{Ae}, \quad (A \neq B), \quad (\text{B10})$$

$$\frac{\partial J_e}{\partial \varepsilon_{Ae}} = J_e, \quad (\text{B11})$$

we arrive at ($A \neq B$, $A \neq C$, $B \neq C$):

$$\frac{\partial \text{dev } \tau_A}{\partial \varepsilon_{Ae}} = \sum_{r=1}^3 (\mu_m)_r (\alpha_m)_r \left(\frac{4}{9} \bar{b}_{Ae}^{(\alpha_m)_r/2} + \frac{1}{9} \bar{b}_{Be}^{(\alpha_m)_r/2} + \frac{1}{9} \bar{b}_{Ce}^{(\alpha_m)_r/2} \right), \quad (\text{B12})$$

$$\frac{\partial \text{dev } \tau_A}{\partial \varepsilon_{Be}} = \sum_{r=1}^3 (\mu_m)_r (\alpha_m)_r \left(-\frac{2}{9} \bar{b}_{Ae}^{(\alpha_m)_r/2} - \frac{2}{9} \bar{b}_{Be}^{(\alpha_m)_r/2} + \frac{1}{9} \bar{b}_{Ce}^{(\alpha_m)_r/2} \right), \quad (\text{B13})$$

$$\frac{\partial(\frac{1}{3} \tau_{NEQ} : \mathbf{1})}{\partial \varepsilon_{Ae}} = K_m J_e^2. \quad (\text{B14})$$

Assuming the viscosities η_D and η_V to be constant, the matrix K_{AB} is given by

$$K_{AB} = \delta_{AB} + \Delta t \frac{1}{2\eta_D} \frac{\partial \text{dev } \tau_A}{\partial \varepsilon_{Be}} - \Delta t \frac{1}{3\eta_V} K_m J_e^2. \quad (\text{B15})$$

APPENDIX C

In this Appendix, it is shown that the algorithmic tangent modulus has the symmetry property

$$C_{AB}^{\text{alg}} = C_{BA}^{\text{alg}}. \quad (\text{C1})$$

By noting the potential structure of

$$\varepsilon_{Ae} = -\Delta t \left(\frac{1}{2\eta_D} \operatorname{dev} \tau_A + \frac{1}{9\eta_V} \tau_{NEQ} : \mathbf{1} \right) + (\varepsilon_{Ae})_{\text{trial}}, \quad (\text{C2})$$

we may write

$$\varepsilon_{Ae} = -\frac{\Delta t}{2\tau} \frac{\partial \Phi_{\text{vis}}}{\partial \tau_A} + (\varepsilon_{Ae})_{\text{trial}}, \quad (\text{C3})$$

which leads to the non-linear equation

$$r_A = \varepsilon_{Ae} + \frac{\Delta t}{2\tau} \frac{\partial \Phi_{\text{vis}}}{\partial \tau_A} - (\varepsilon_{Ae})_{\text{trial}} = 0. \quad (\text{C4})$$

Linearizing with respect to the logarithmic strains yields

$$r_A = \bar{r}_A + \Delta r_A \approx 0 \Rightarrow \underbrace{\left(\delta_{AC} + \frac{\Delta t}{2\tau} \frac{\partial^2 \Phi_{\text{vis}}}{\partial \tau_A \partial \tau_B} \frac{\partial \tau_B}{\partial \varepsilon_{Ce}} \right)}_{K_{AC}} \Delta \varepsilon_{Ce} = -\bar{r}_A. \quad (\text{C5})$$

Note that the summation convention is assumed to hold in (C5) and below. The algorithmic tangent modulus C_{AB}^{alg} is calculated as

$$\begin{aligned} C_{AB}^{\text{alg}} &= \frac{\partial \tau_A}{\partial \varepsilon_{Ce}} (K_{BC})^{-1} \\ &= \frac{\partial \tau_A}{\partial \varepsilon_{Ce}} \left(\delta_{BC} + \frac{\Delta t}{2\tau} \frac{\partial^2 \Phi_{\text{vis}}}{\partial \tau_B \partial \tau_D} \frac{\partial \tau_D}{\partial \varepsilon_{Ce}} \right)^{-1} \\ &= \frac{\partial \tau_A}{\partial \varepsilon_{Ce}} \left(\left(\frac{\partial \tau_D}{\partial \varepsilon_{Be}} \right)^{-1} \frac{\partial \tau_D}{\partial \varepsilon_{Ce}} + \frac{\Delta t}{2\tau} \frac{\partial^2 \Phi_{\text{vis}}}{\partial \tau_B \partial \tau_D} \frac{\partial \tau_D}{\partial \varepsilon_{Ce}} \right)^{-1} \\ &= \frac{\partial \tau_A}{\partial \varepsilon_{Ce}} \left(\left[\left(\frac{\partial \tau_D}{\partial \varepsilon_{Be}} \right)^{-1} + \frac{\Delta t}{2\tau} \frac{\partial^2 \Phi_{\text{vis}}}{\partial \tau_B \partial \tau_D} \right] \frac{\partial \tau_D}{\partial \varepsilon_{Ce}} \right)^{-1} \\ &= \underbrace{\frac{\partial \tau_A}{\partial \varepsilon_{Ce}} \left(\frac{\partial \tau_D}{\partial \varepsilon_{Ce}} \right)^{-1}}_{\delta_{AD}} \left(\left(\frac{\partial \tau_D}{\partial \varepsilon_{Be}} \right)^{-1} + \frac{\Delta t}{2\tau} \frac{\partial^2 \Phi_{\text{vis}}}{\partial \tau_B \partial \tau_D} \right)^{-1} \\ &= \left(\left(\frac{\partial \tau_A}{\partial \varepsilon_{Be}} \right)^{-1} + \frac{\Delta t}{2\tau} \frac{\partial^2 \Phi_{\text{vis}}}{\partial \tau_B \partial \tau_A} \right)^{-1}. \end{aligned} \quad (\text{C6})$$

For sufficiently smooth potentials Φ_{vis} the second partial derivatives may be interchanged; i.e.

$$\frac{\partial^2 \Phi_{\text{vis}}}{\partial \tau_A \partial \tau_B} = \frac{\partial^2 \Phi_{\text{vis}}}{\partial \tau_B \partial \tau_A}. \quad (\text{C7})$$

Further, because of the existence of the potential Ψ_{NEQ} , we have that

$$\frac{\partial \tau_A}{\partial \varepsilon_{Be}} = \frac{\partial \tau_B}{\partial \varepsilon_{Ae}}. \quad (\text{C8})$$

Thus, we may conclude from (C6)–(C8) that

$$C_{AB}^{\text{alg}} = C_{BA}^{\text{alg}}. \quad (\text{C9})$$